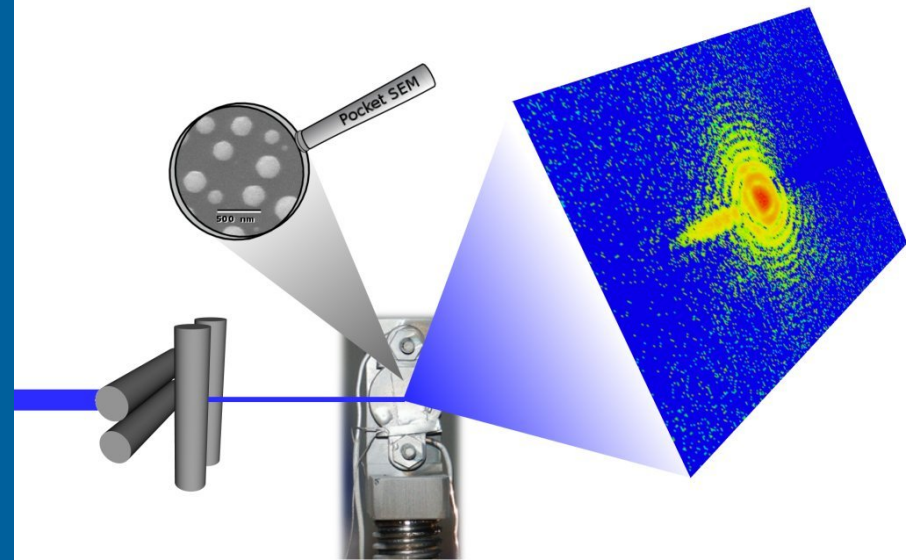


WE START WITH YES.

DEVELOPMENT OF IN-SITU
BROADBAND LAUE
MICRODIFFRACTION FOR
DETERMINATION OF
CRYSTALLOGRAPHIC ORIENTATION AT
THE 34-ID-C BRAGG COHERENT
DIFFRACTION IMAGING INSTRUMENT



DR. ROSS HARDER
Advanced Photon Source
Argonne National Laboratory

Beamline 34-ID-C

MULTI INSTITUTION PARTNERSHIP

PUP began in 2017 with LANL

Richard Sandberg, Brigham Young University

Saryu Fensin, Los Alamos National Laboratory

Reeju Pokharel, Los Alamos National Laboratory

Jonathan Gigax, Los Alamos National Laboratory

Ross Harder, Advanced Photon Source

Wonsuk Cha, Advanced Photon Source

Jon Tischler, Advanced Photon Source

Wenjun Liu, Advanced Photon Source

Tony Rollett, Carnegie Mellon University

Anastasios Pateras, Carnegie Mellon University

Matthew Wilkin, Carnegie Mellon University

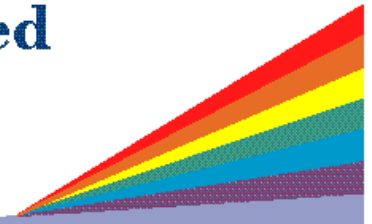
Yueheng Zhang, Carnegie Mellon University



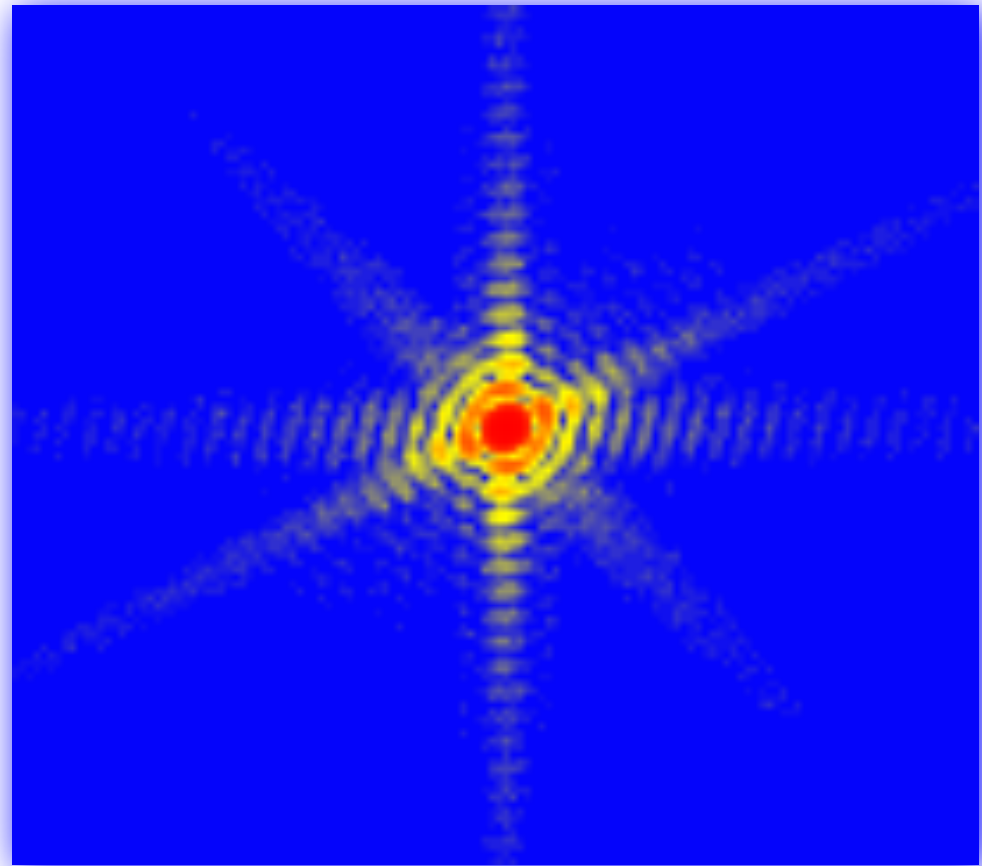
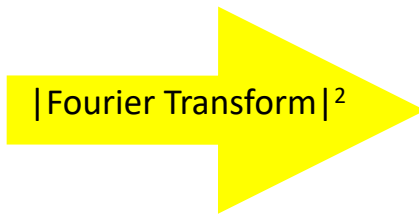
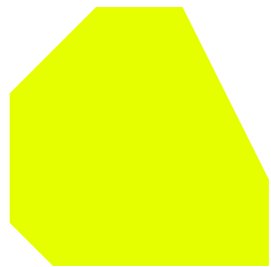
**Carnegie
Mellon
University**



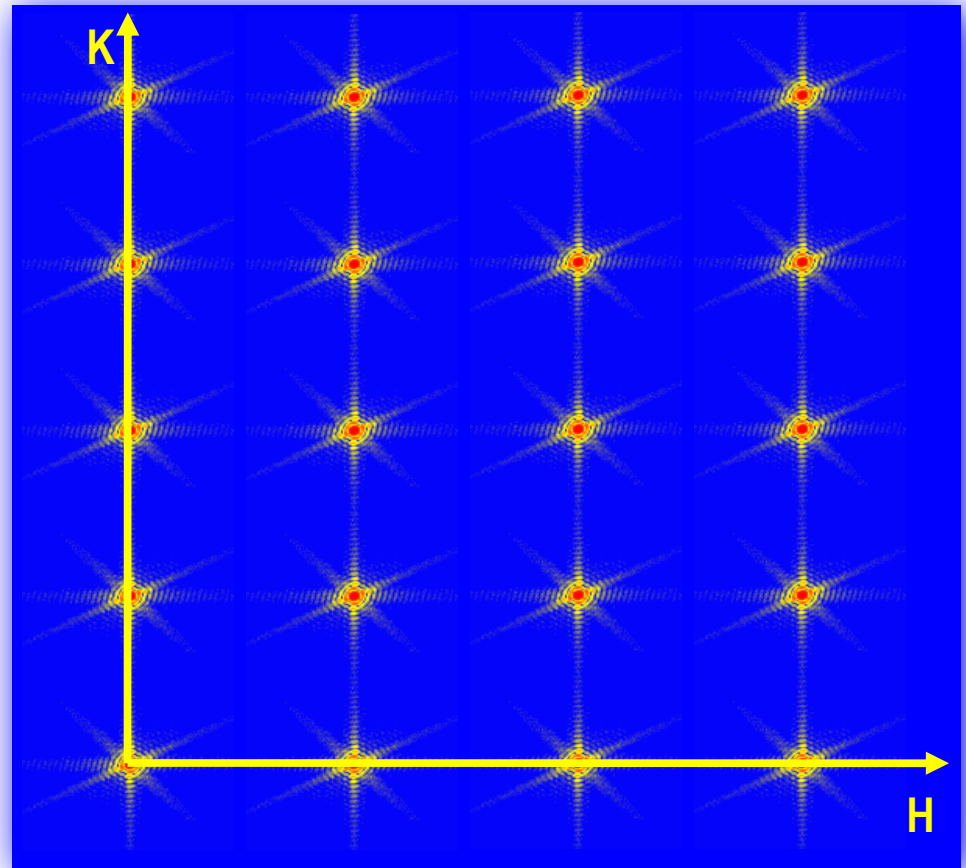
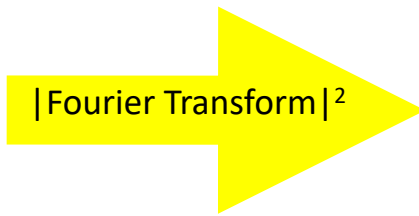
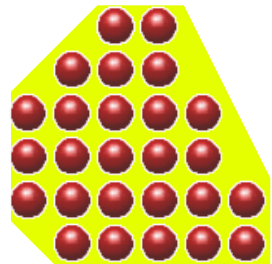
**Advanced
Photon
Source**



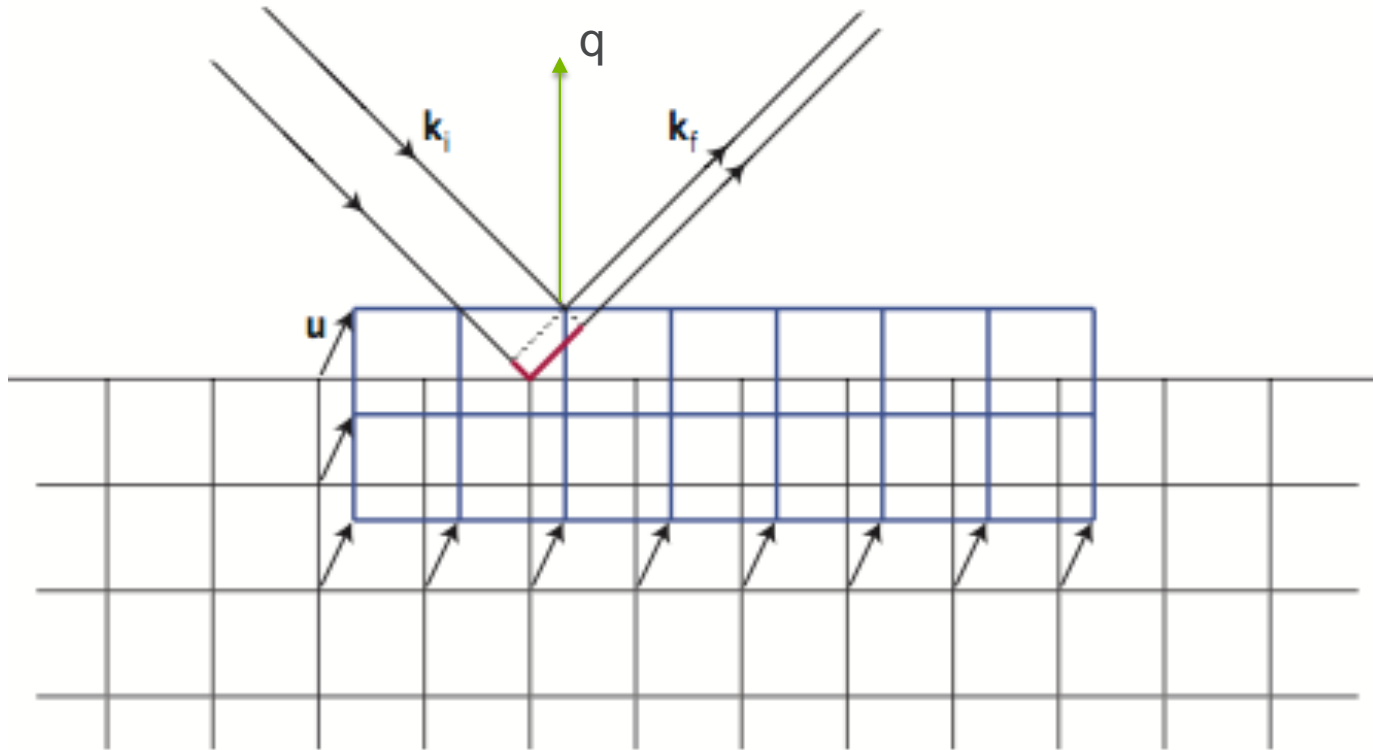
Coherent Diffraction from Crystals



Coherent Diffraction from Crystals

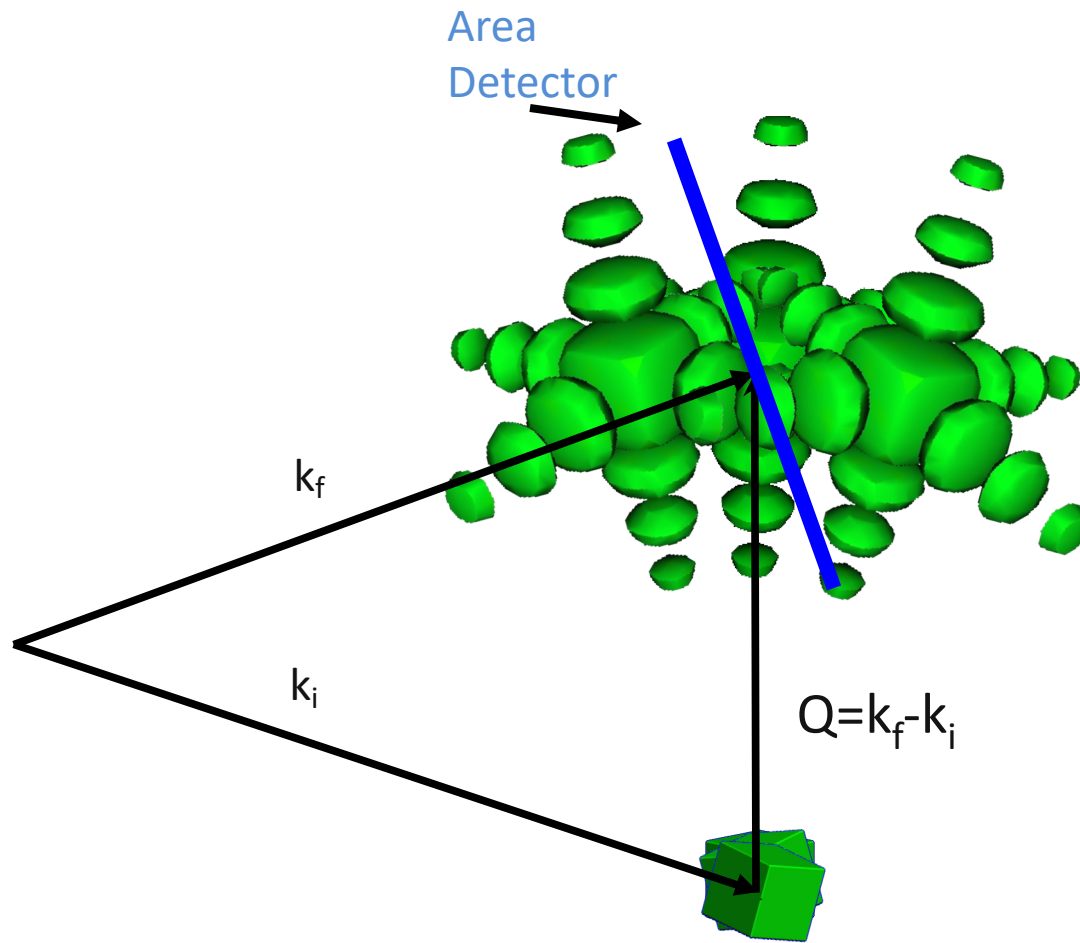


STRUCTURAL SENSITIVITY WITH BRAGG CDI

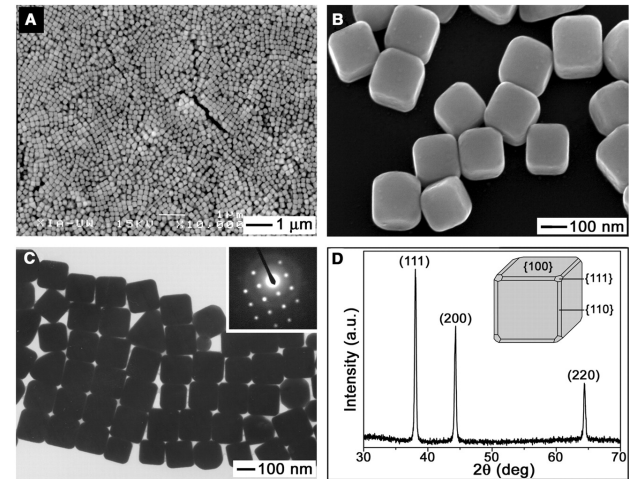
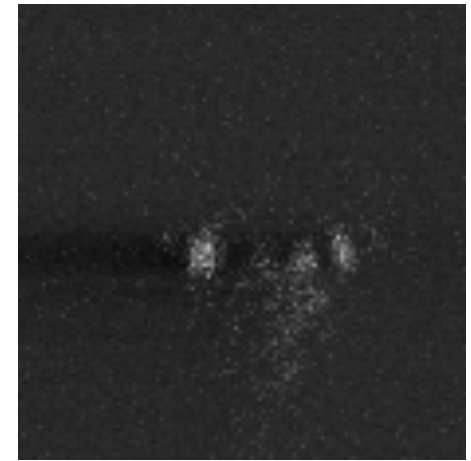


Measured intensity affected by atomic displacement fields with picometer sensitivity

Measuring 3D CXD

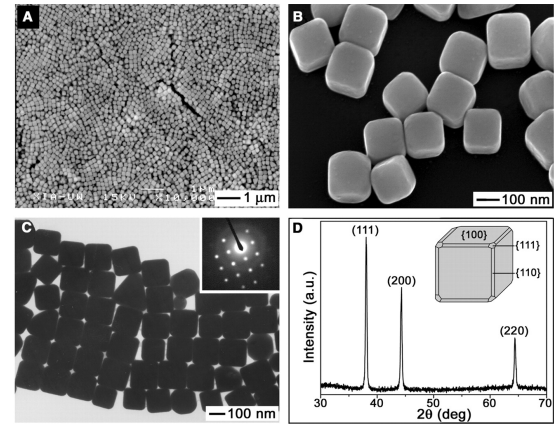
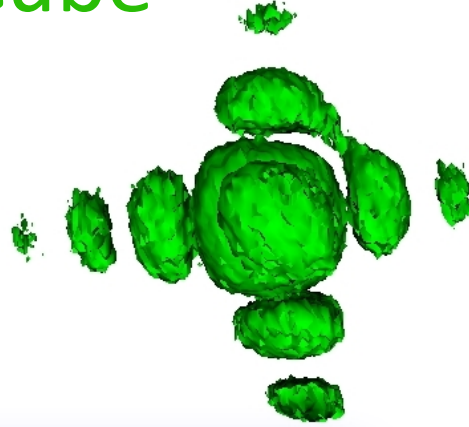
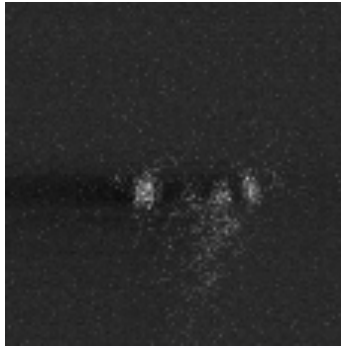


Silver Nano Cube (111)

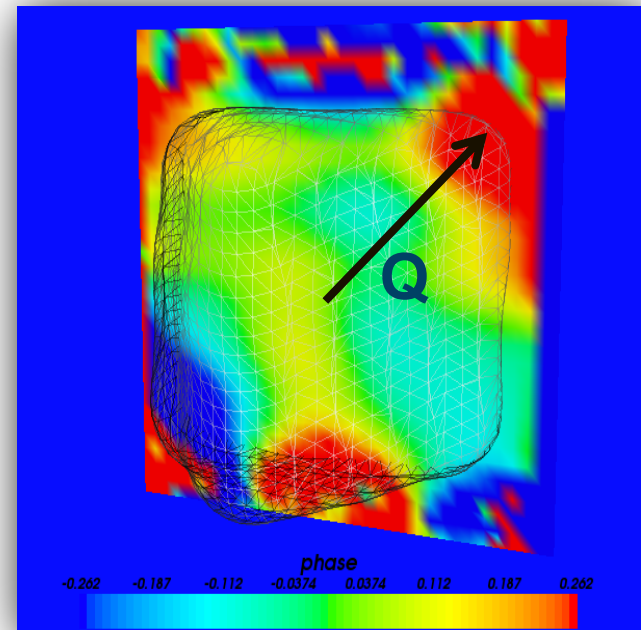
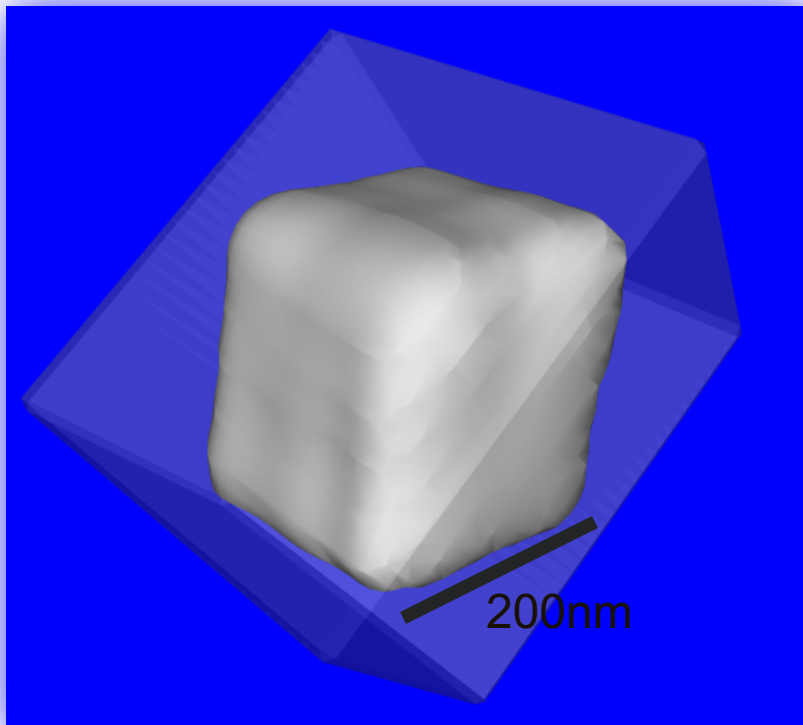


Yugang Sun and Younan Xia,
Science 298 2177 (2003)

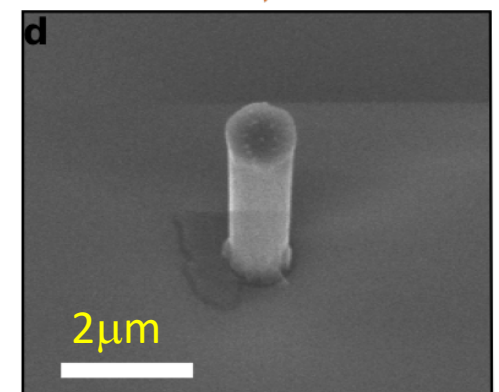
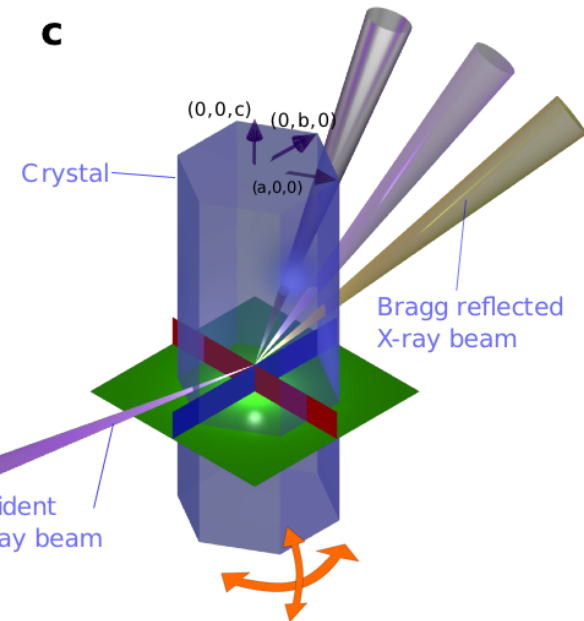
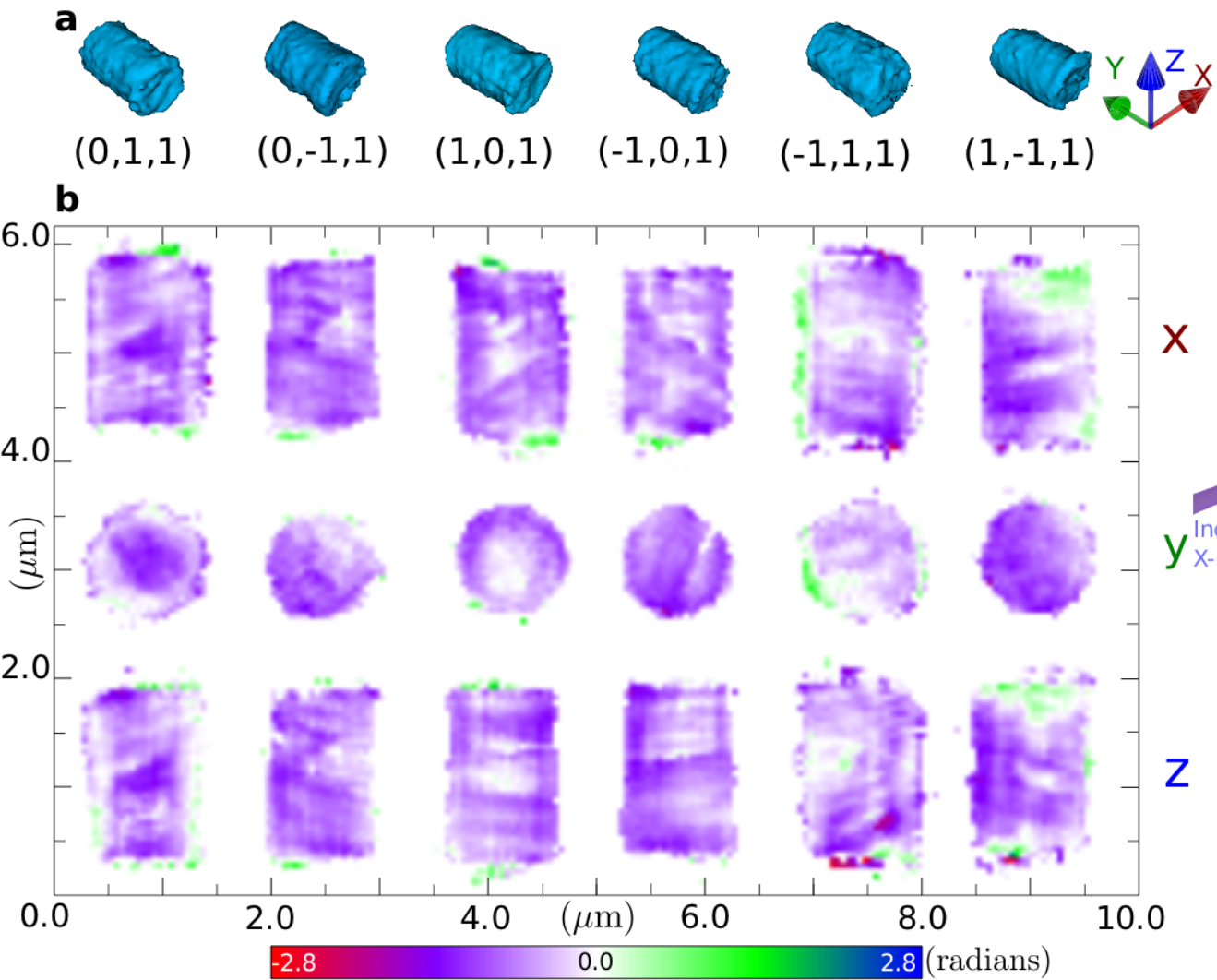
3D Ag Nano Cube



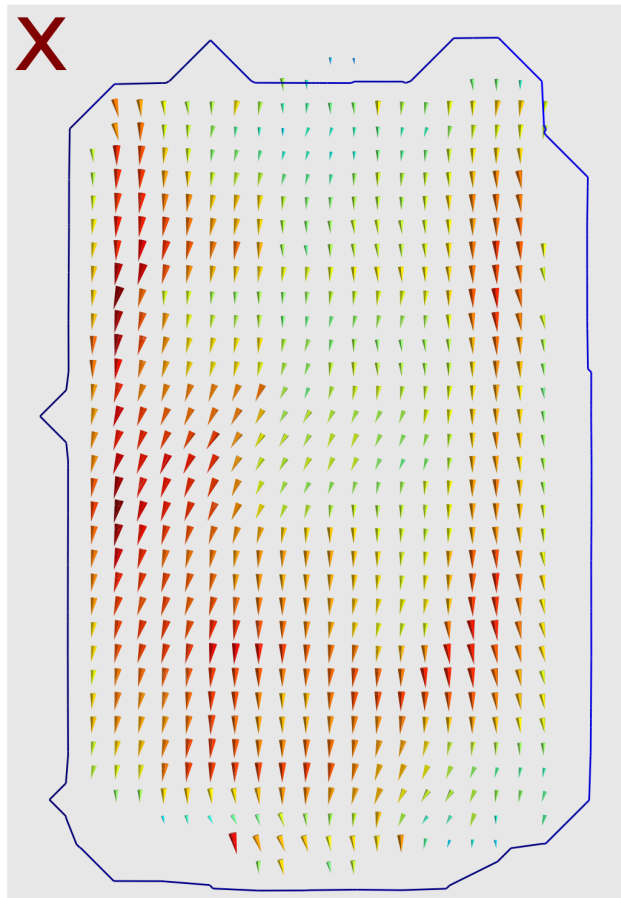
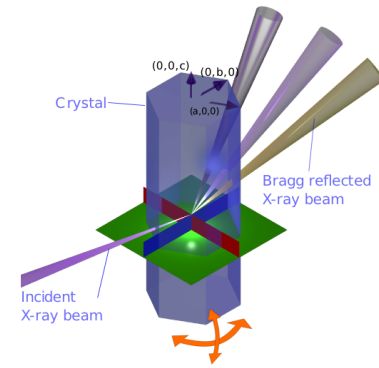
Yugang Sun and Younan Xia,
Science 298 2177 (2003)



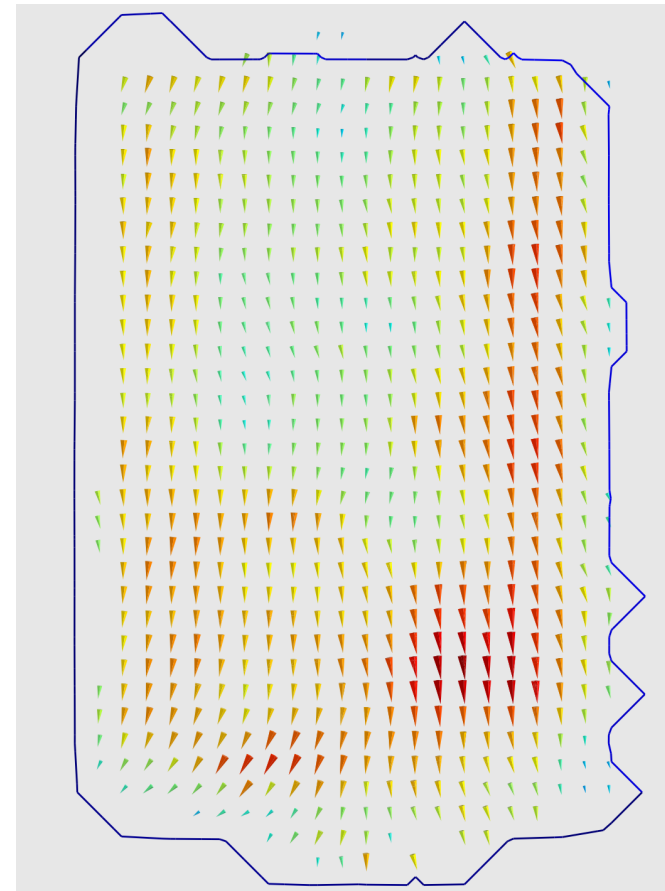
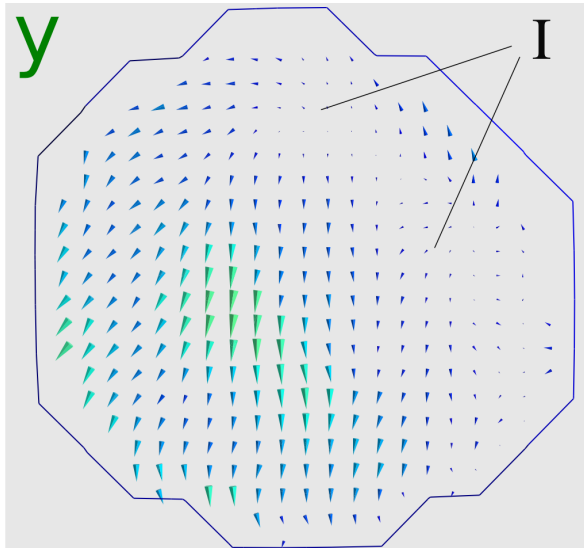
3D Strain Map in ZnO



3D Strain Map in ZnO



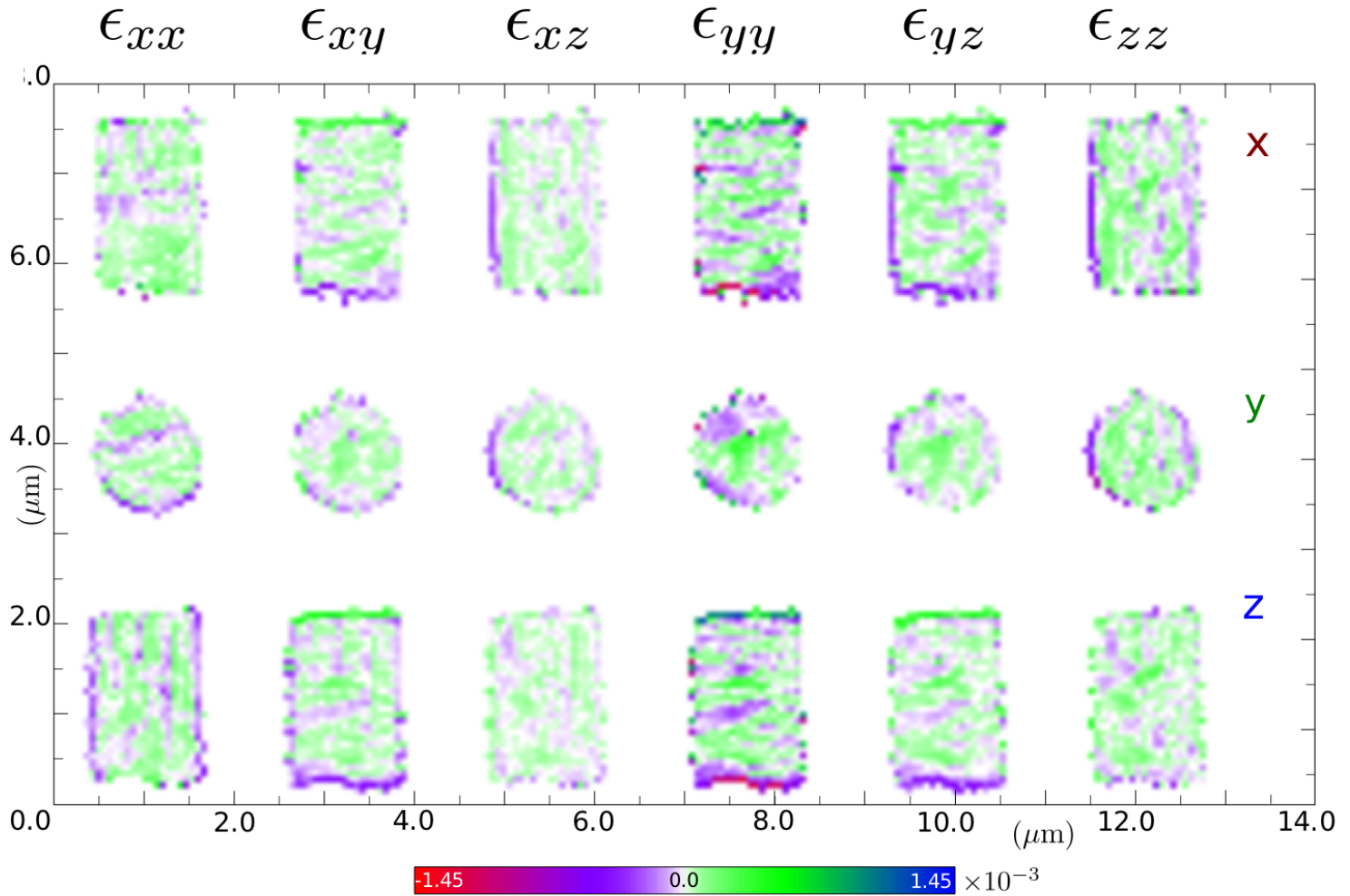
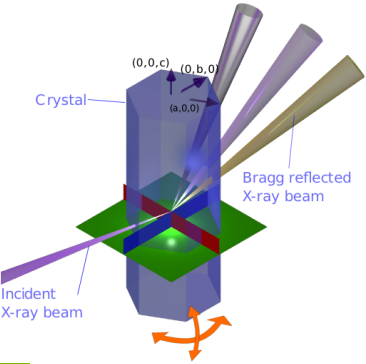
$$u_j = \xi_{ji} q_{ki} \phi_k; \quad \xi_{ji} = (q_{kj} q_{ki})^{-1}$$



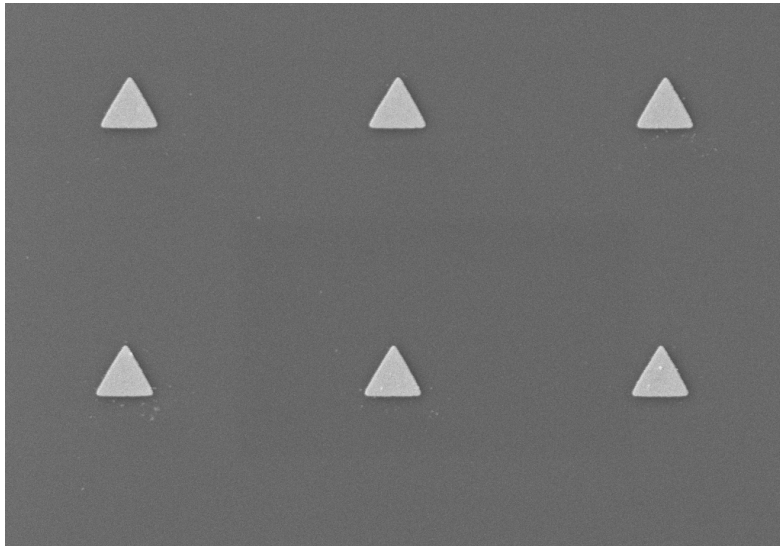
0.0 0.09 nm

3D Strain Map in ZnO

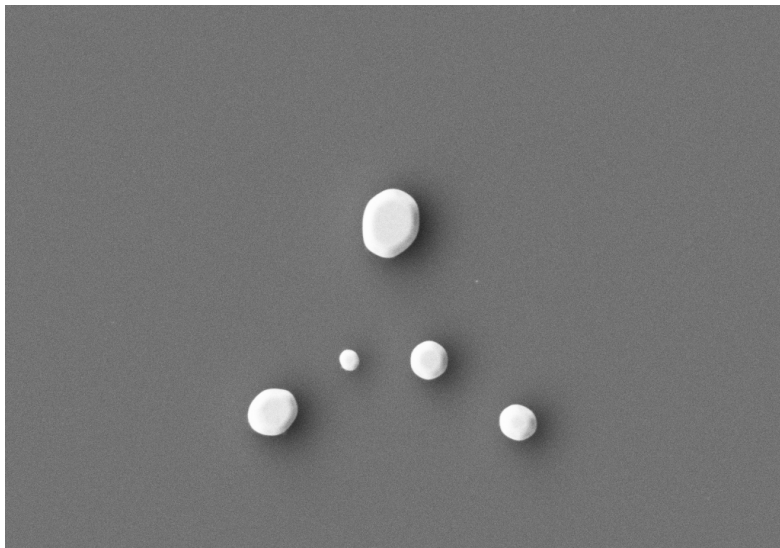
$$\epsilon_{ij} = \frac{1}{2} \left(\frac{\partial u_j}{\partial x_i} + \frac{\partial u_i}{\partial x_j} \right), \quad \tau_{ij} = \left(\frac{\partial u_j}{\partial x_i} - \frac{\partial u_i}{\partial x_j} \right)$$



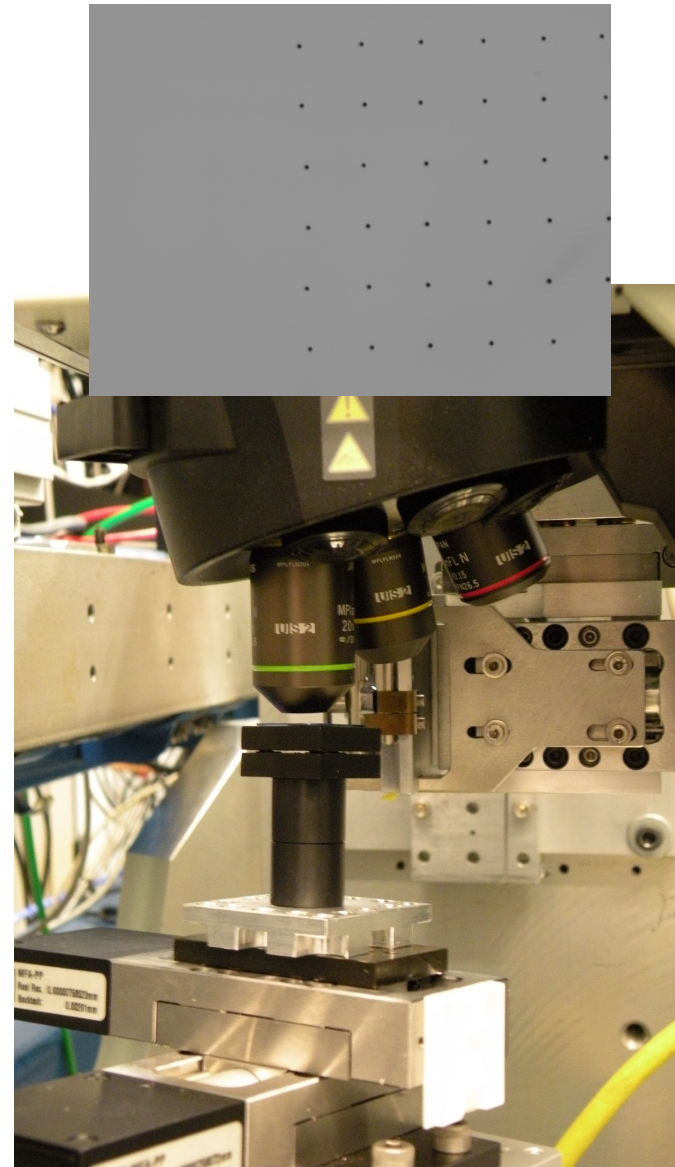
Patterned Gold Nanocrystal Samples



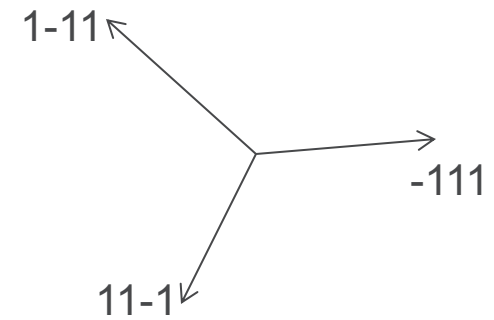
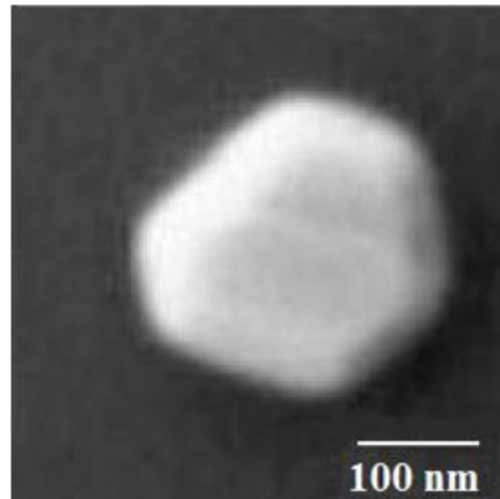
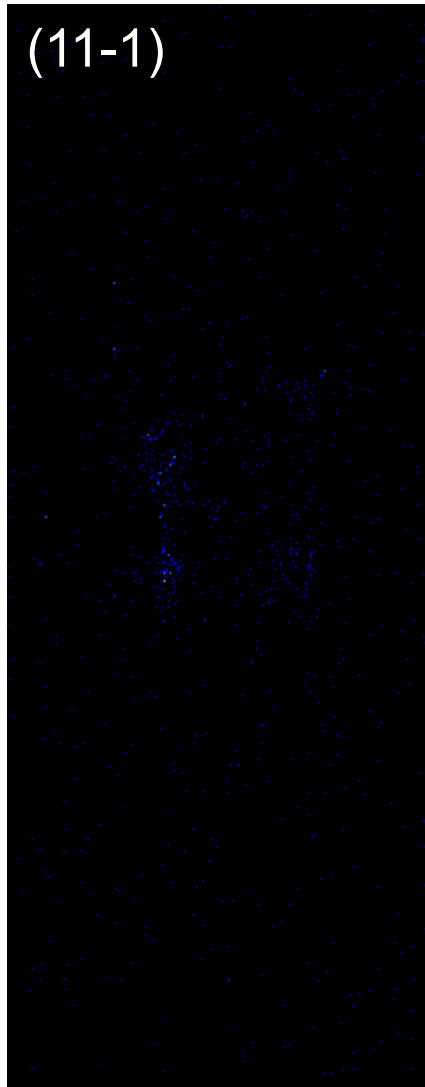
Mag = 7.04 K X 1 μm WD = 17.0 mm EHT = 5.00 kV FIB Lock Mags = No Signal A = SE2 Date :20 Jan 2009 Time :17:50:43
1540XB-27-20 FIB Imaging - SEM Noise Reduction = Line Avg FIB Probe = 30KV-2 pA System Vacuum = 1.85e-006 mbar



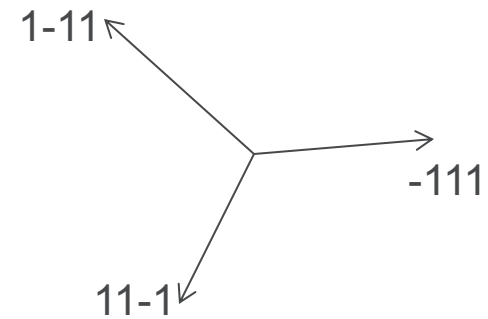
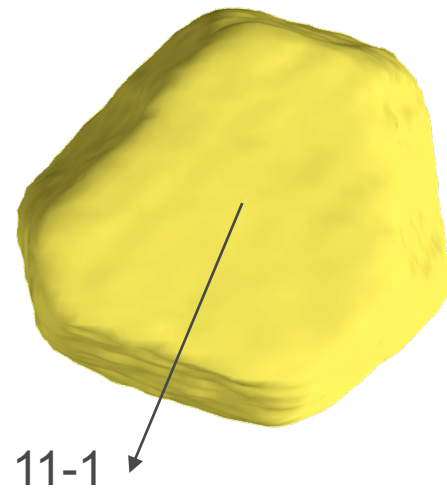
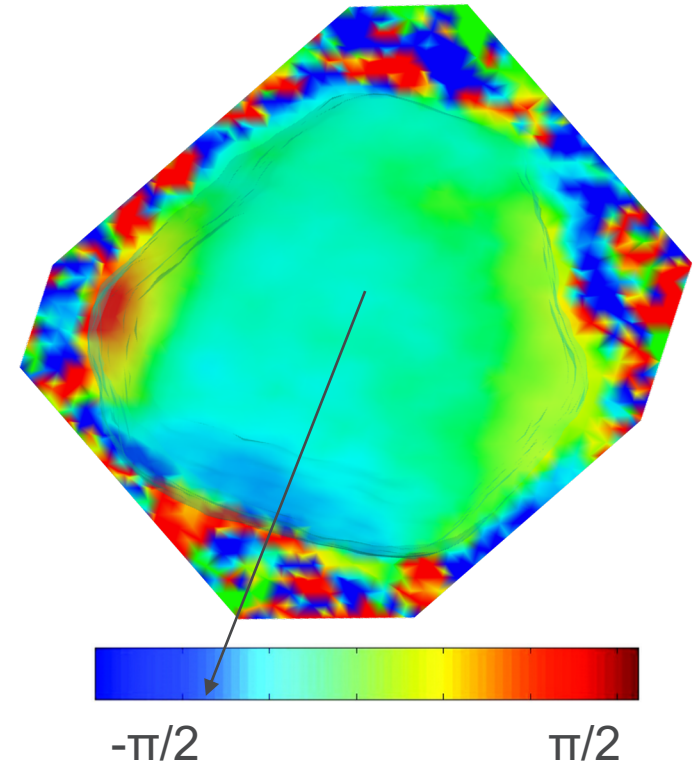
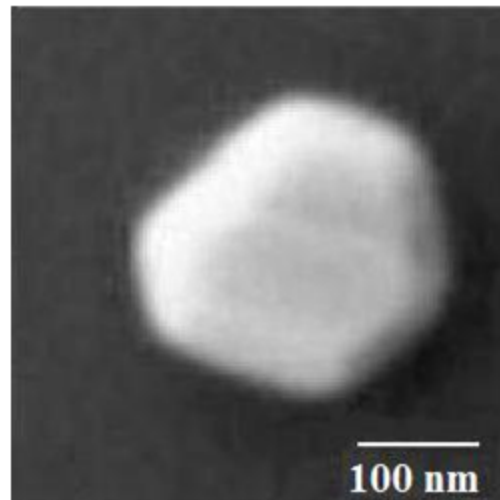
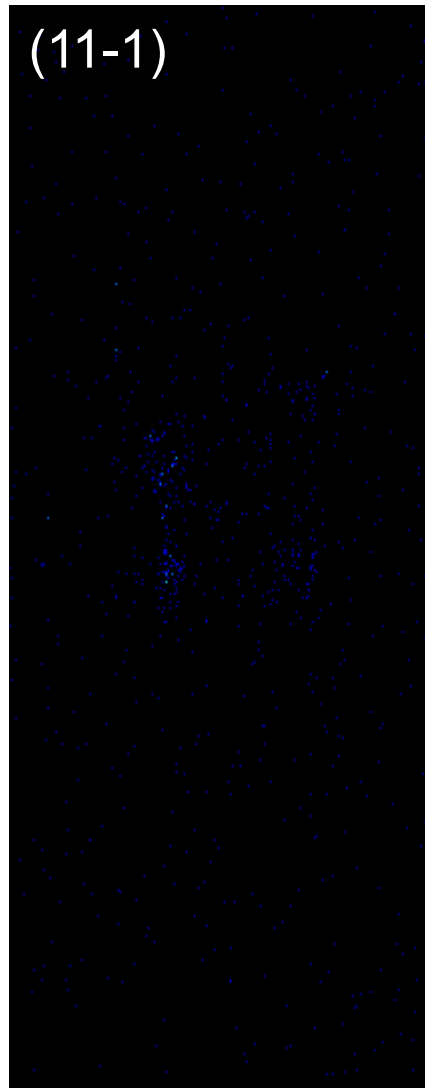
Mag = 45.53 K X 200 nm WD = 5.5 mm EHT = 5.00 kV FIB Lock Mags = No Signal A = SE2 Date :18 Nov 2008 Time :14:51:11
1540XB-27-20 FIB Imaging - SEM Noise Reduction = Line Avg FIB Probe = 30KV-2 pA System Vacuum = 3.52e-006 mbar



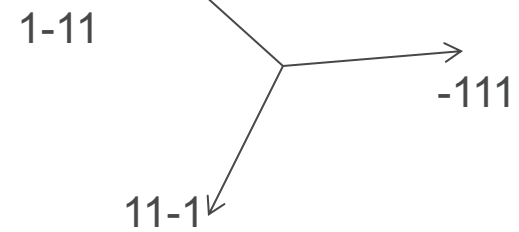
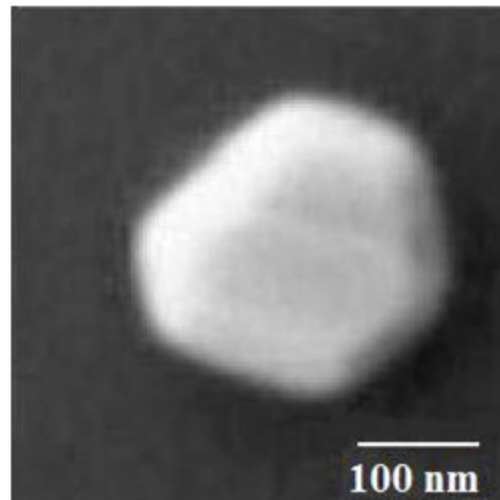
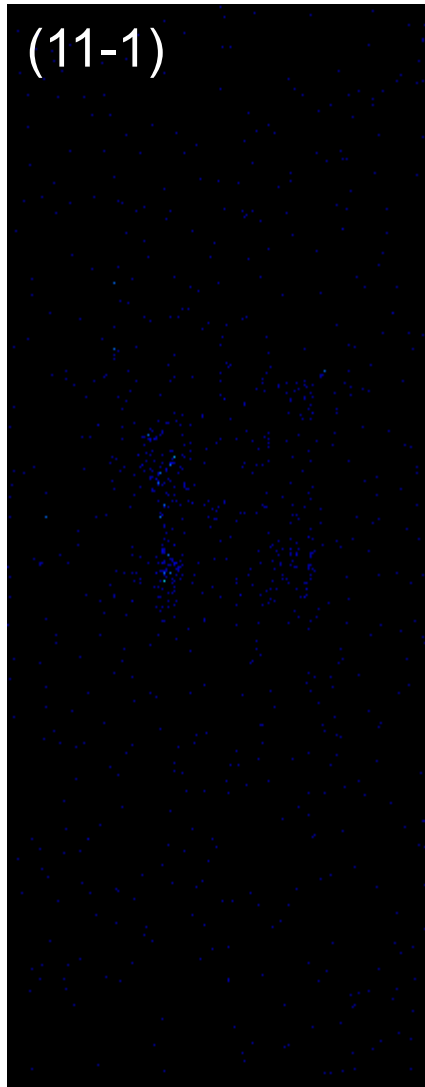
Multiple reflection reconstructions



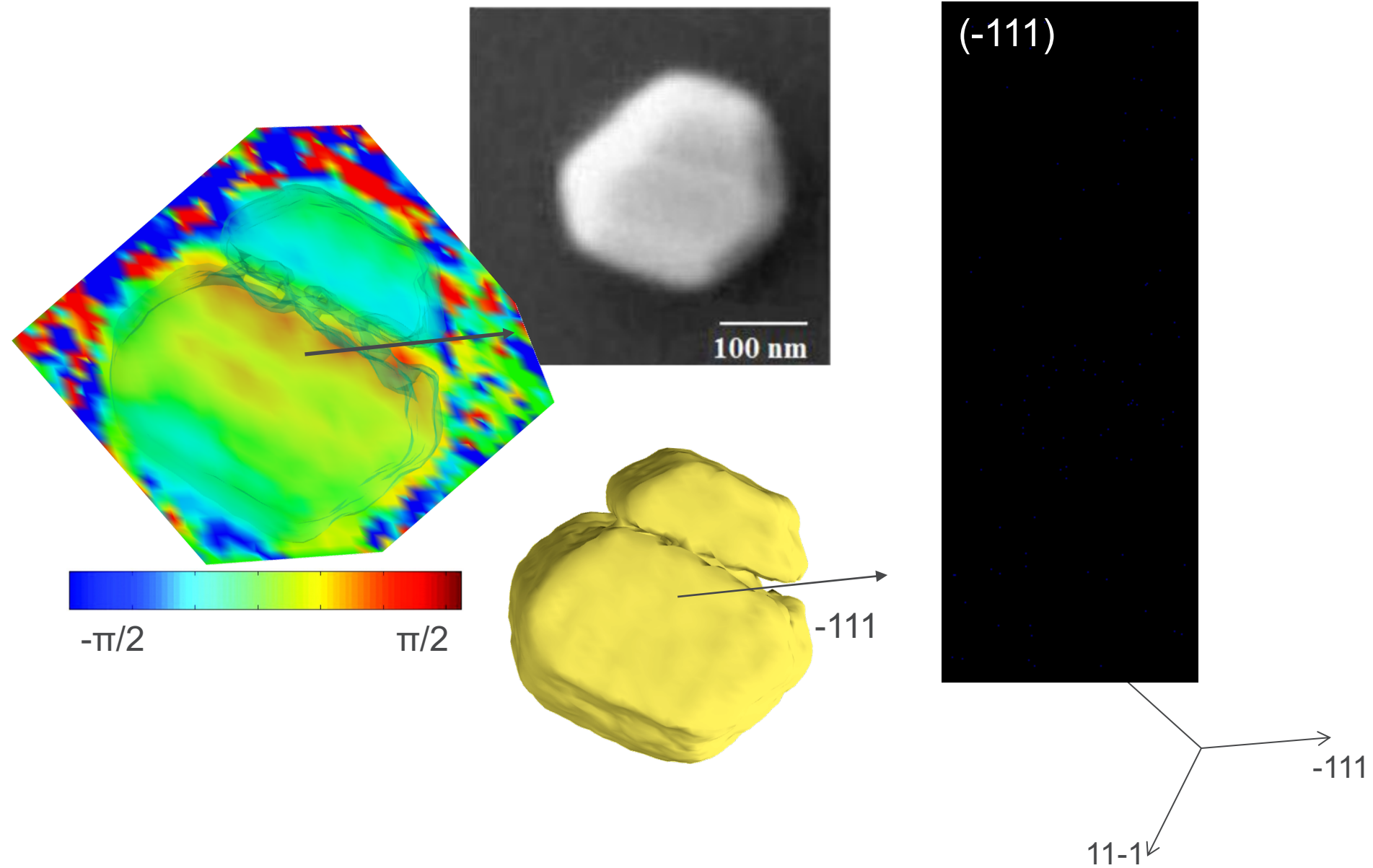
Multiple reflection reconstructions



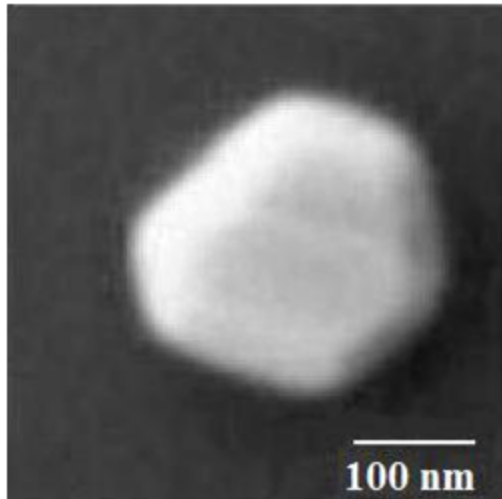
Multiple reflection reconstructions



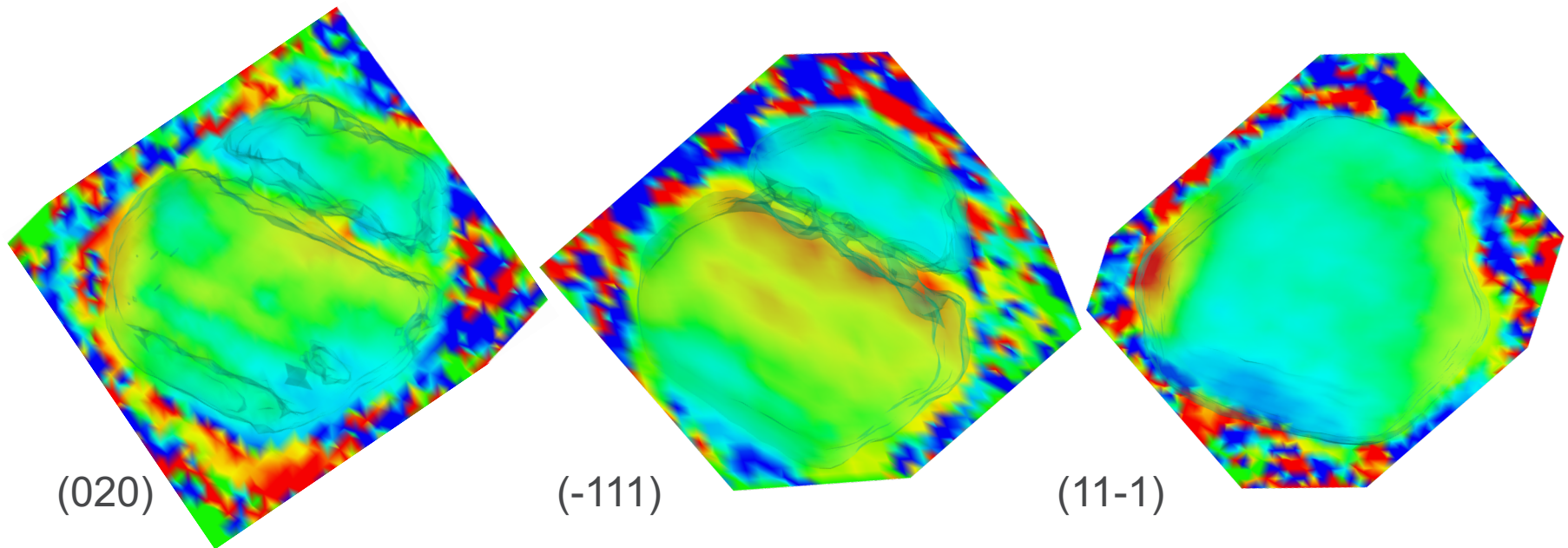
Multiple reflection reconstructions



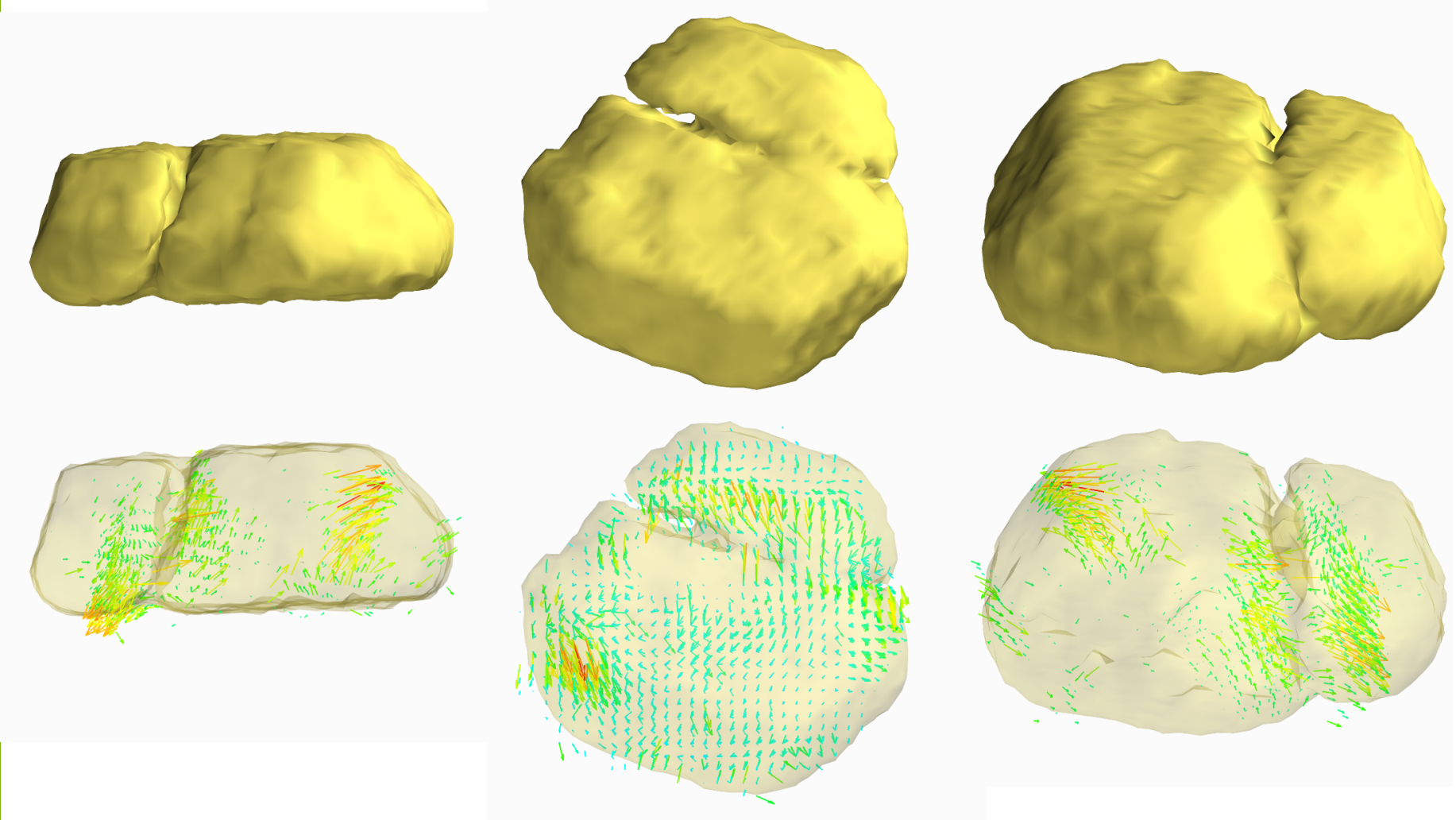
Multiple reflection reconstructions



$$\varphi = q \cdot u(r)$$

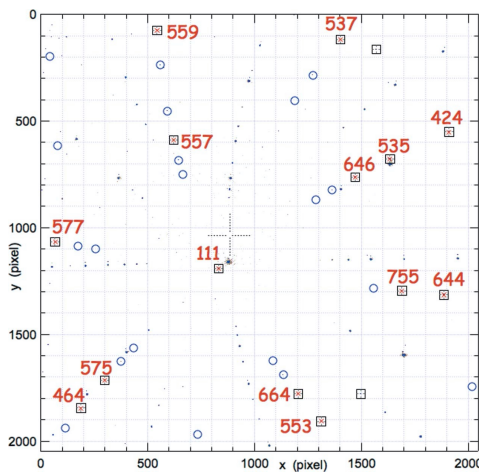
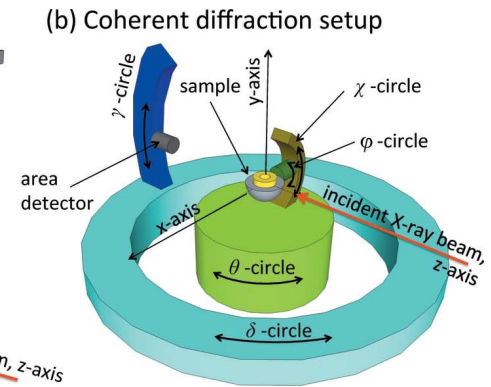
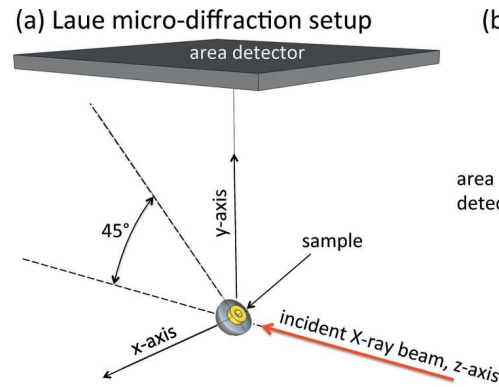
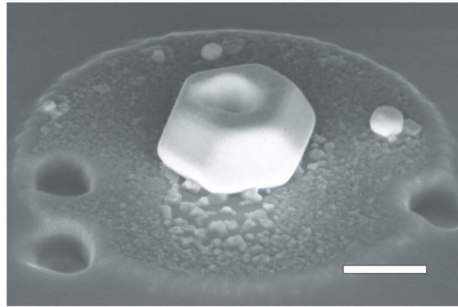


Vector Displacement Field of Gold lattice

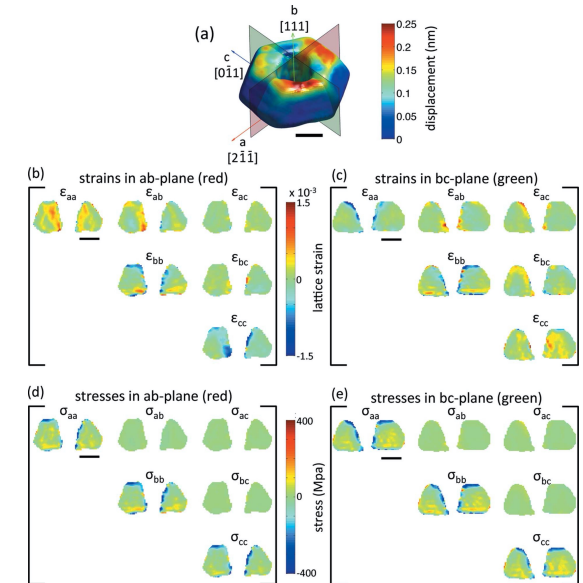
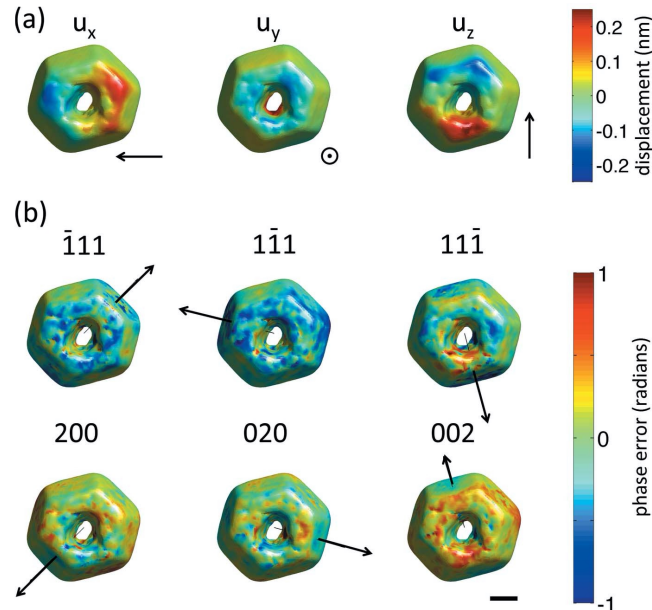


Produced by combining images from (11-1) (020) (-111)

LAUE @ 34-ID-E BCDI @ 34-ID-C

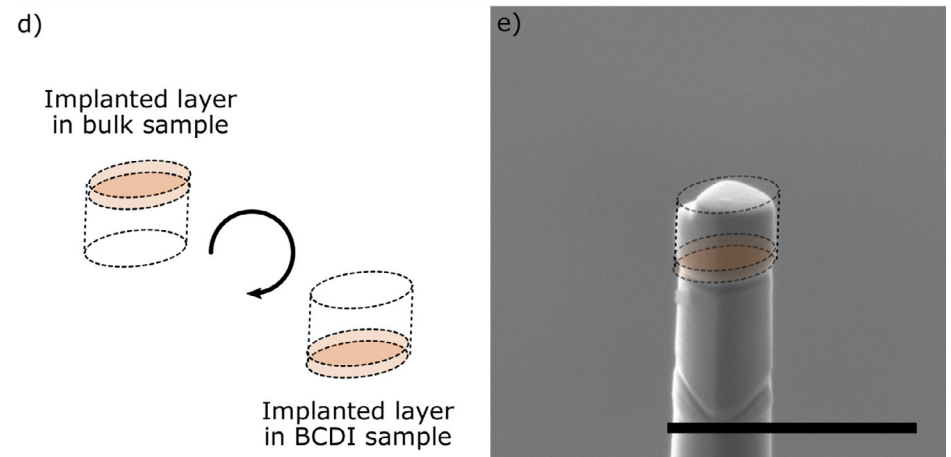
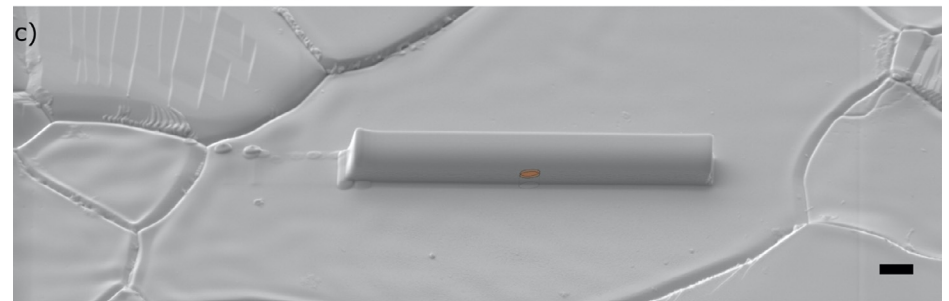
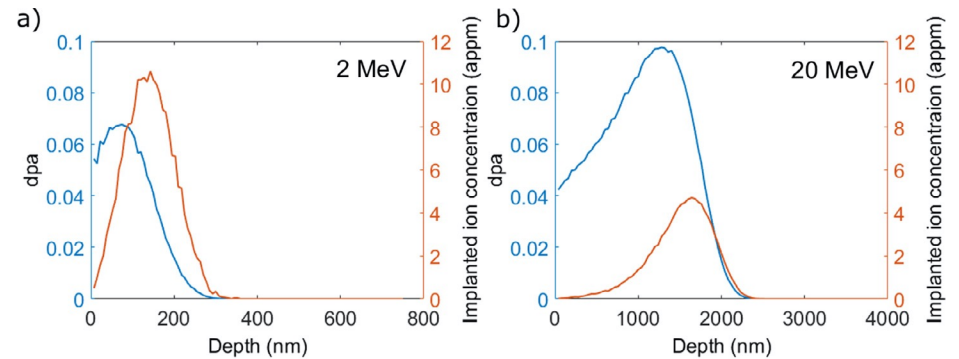
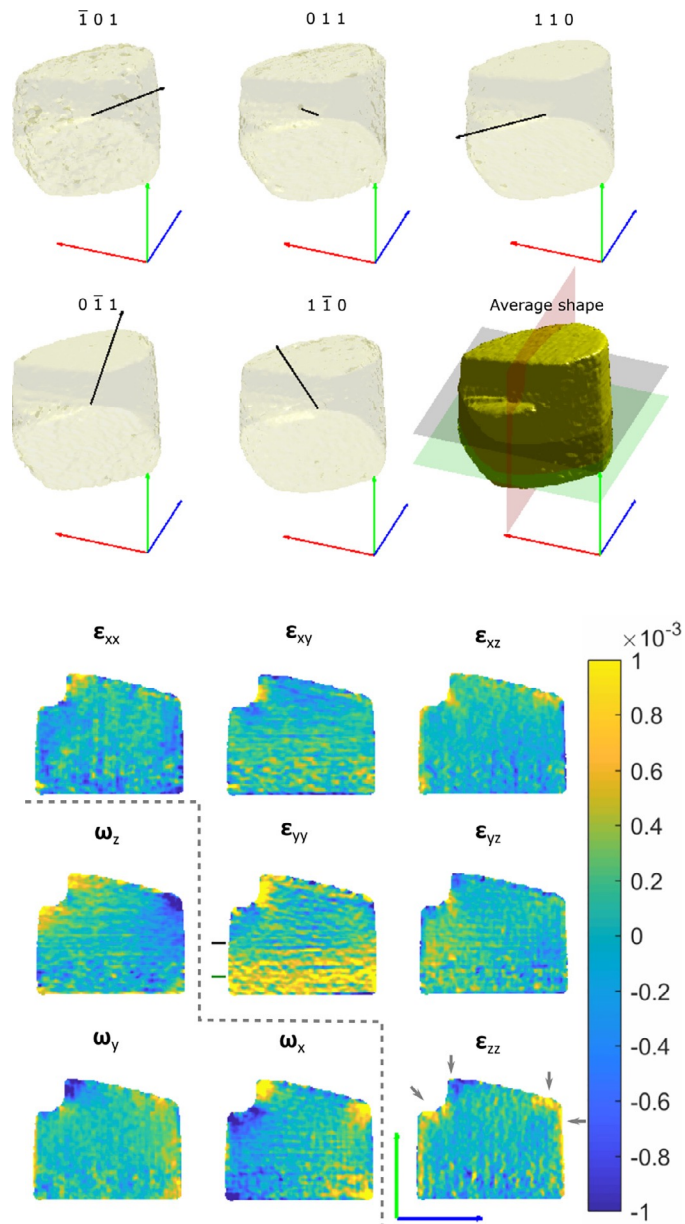


reciprocal lattice vectors:
 $a^* \ b^* \ c^*$
 $-6.773459 \ +0.130656 \ -9.377983$
 $+1.778382 \ +11.375979 \ -1.125984$
 $+9.208746 \ -2.100812 \ -6.680493$

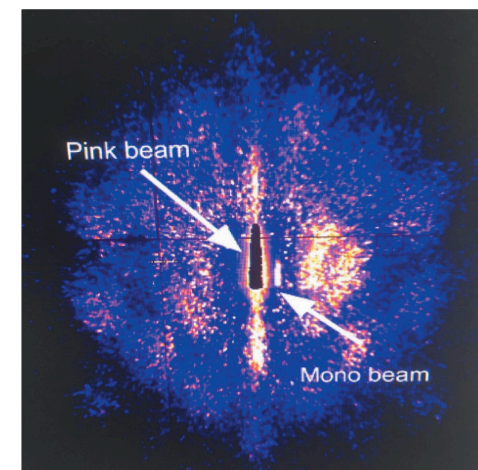
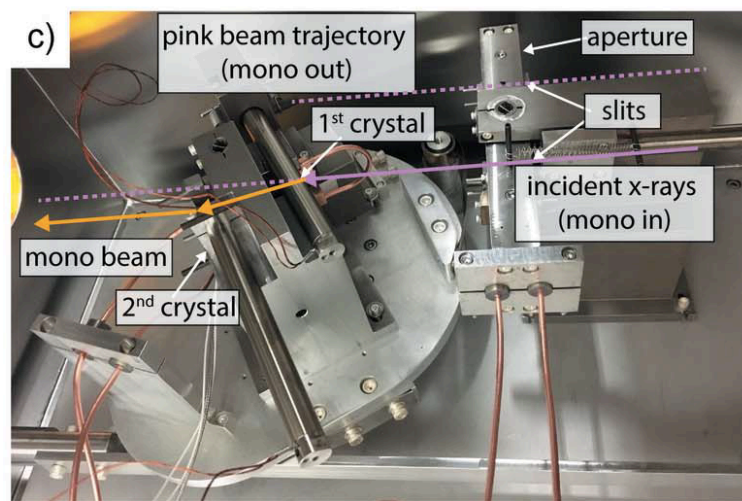
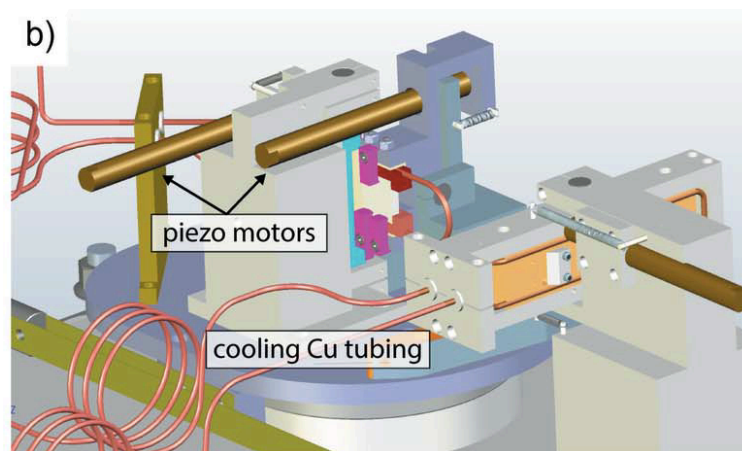
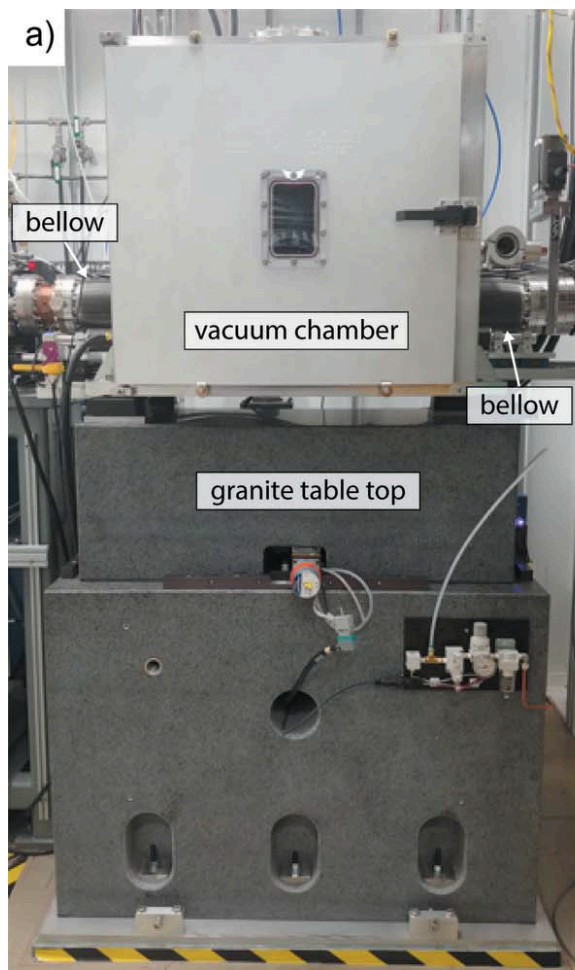


Nanoscale lattice strains in self-ion implanted tungsten

Phillips, N. W., et al. (2020). *Acta Materialia*. **195**, 219–228.

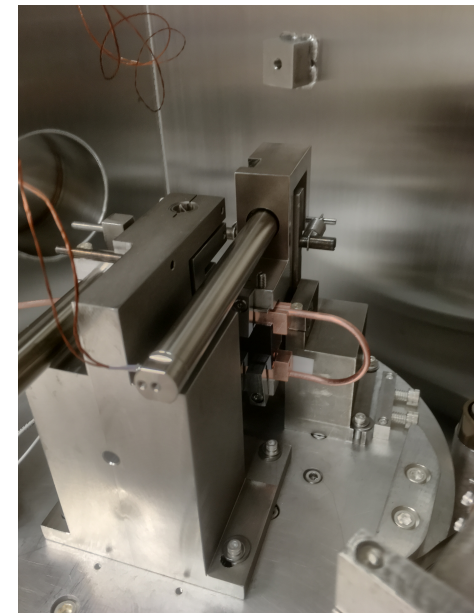
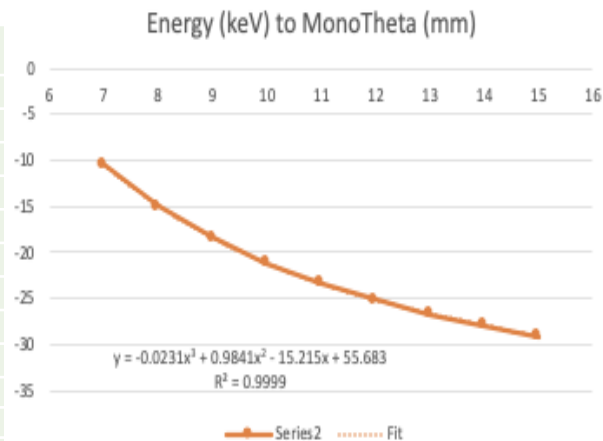


Commissioning of a movable double-bounce monochromator at 34-ID-C



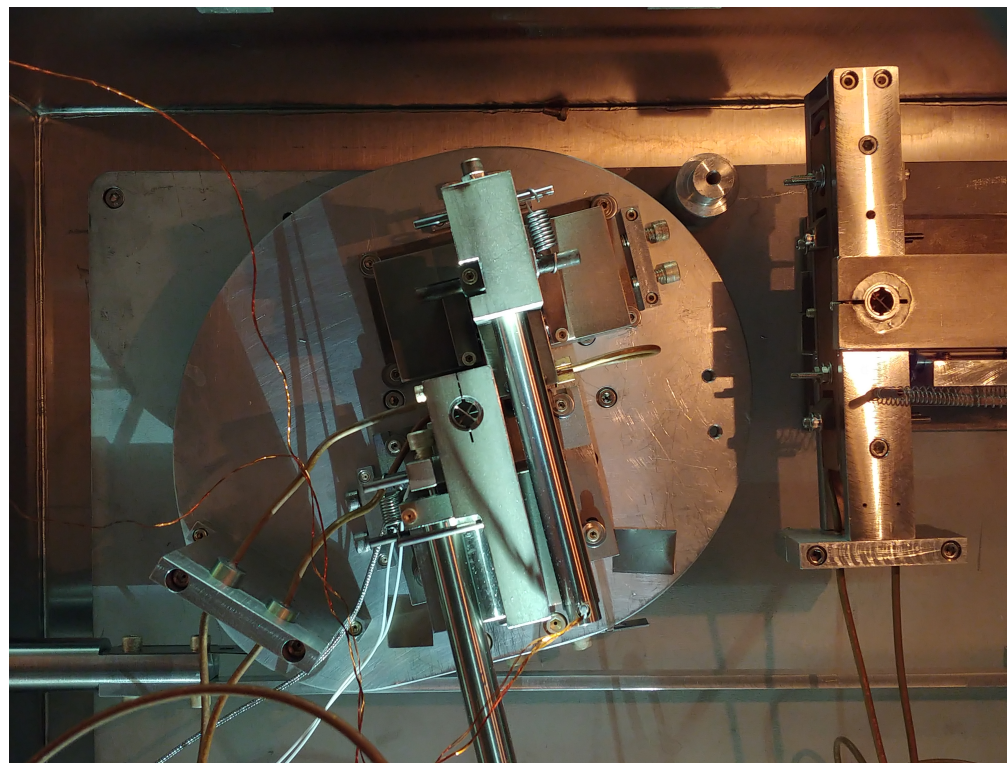
Energy Calibration

Energy (keV)	mcr (degree)	MonoTable (mm)
7	16.407	-10.4625
8	14.309	-15.0225
9	12.691	-18.4238
10	11.403	-21.1275
11	10.355	-23.315
12	9.4835	-25.1388
13	8.748	-26.665
14	8.1188	-27.965
15	7.5743	-29.1275



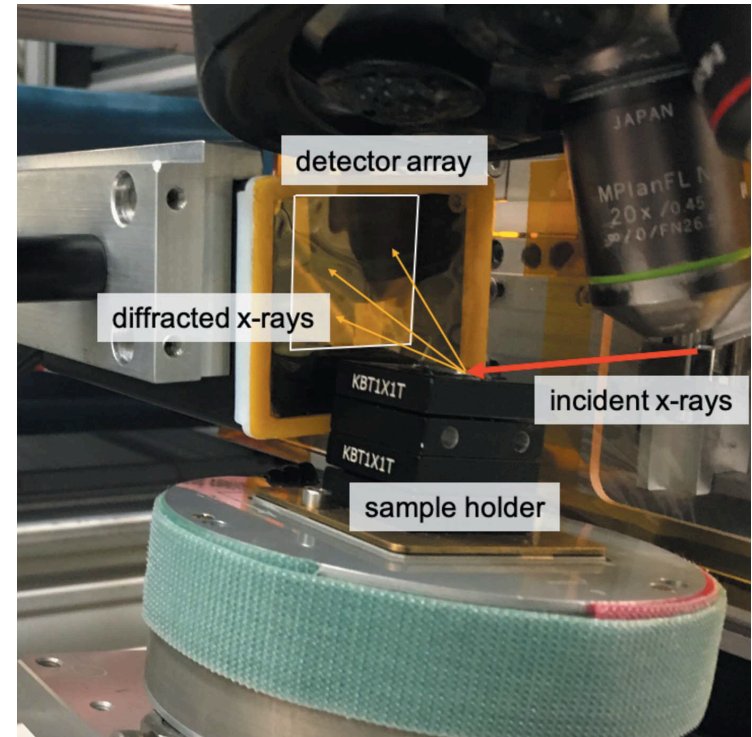
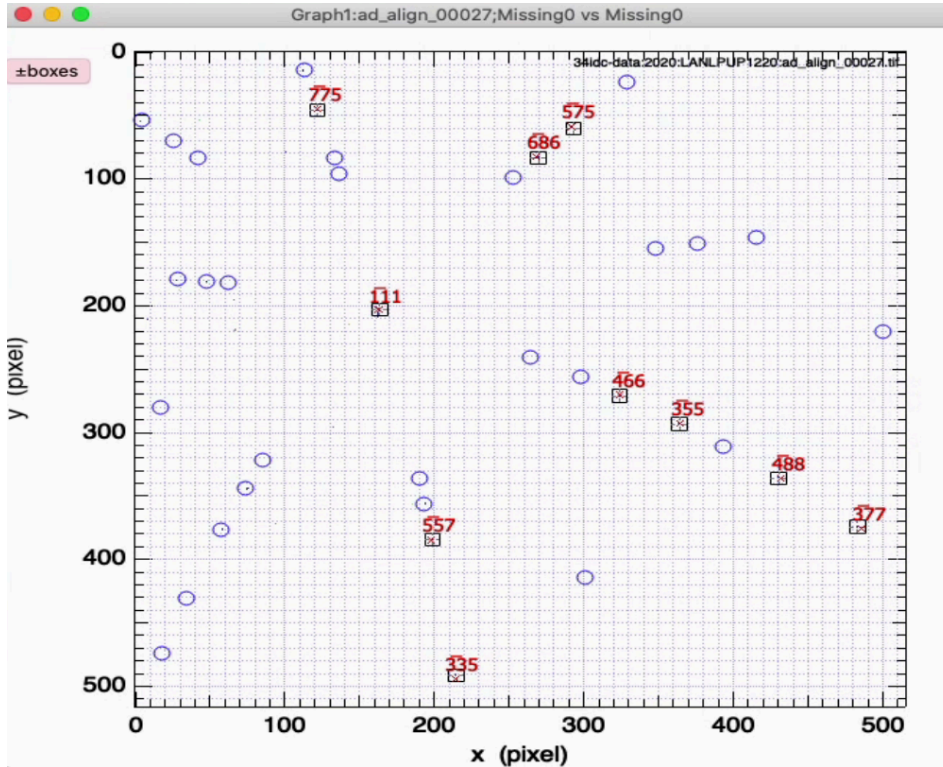
$$y = -0.0231x^3 + 0.9841x^2 - 15.215x + 55.683$$

Energy (keV)	MonoTheta		Δ MonoTheta
	MonoTheta Cal.	Meas.	
7	-10.5244	-10.4625	0.0619
8	-14.8818	-15.0225	-0.1407
9	-18.3798	-18.4238	-0.044
10	-21.157	-21.1275	0.0295
11	-23.352	-23.315	0.037
12	-25.1034	-25.1388	-0.0354
13	-26.5498	-26.665	-0.1152
14	-27.8298	-27.965	-0.1352
15	-29.082	-29.1275	-0.0455



Laue Detector Calibration with Energy using LaueGo

Manually optimized R and P and saved in *geoN_2020-12-10_10-23-48.xml*



OptimizeAll(CalibrationList_000270,\$"", "\$"")

Nenergies = 5

Detector 0

started at $\mathbf{R}=\{1.2092, 1.2092, 1.2092\}$, $\mathbf{P}=\{16.95, 0, -27.16\}$ mm, $|\mathbf{R}| = 120^\circ$

sample started at axis = $\{3.00763, -0.0430946, -1.66093\}$, $|\text{sample angle}| = 196.871^\circ$

ended at $\mathbf{R}=\{1.21684, 1.20658, 1.21452\}$, $\mathbf{P}=\{17.329, 0.501, -27.648\}$ mm, $|\mathbf{R}| = 120.343^\circ$

final sample rotation is $\{2.98265, -0.0436981, -2.71797\}$, $|\text{sample angle}| = 231.219^\circ$,

$\Delta\rho = \{-0.025, -0.0006, -1.1\}$, $|\Delta\rho|=61^\circ$

error started at 0.44055, reduced to 0.00272677, after 64 iterations

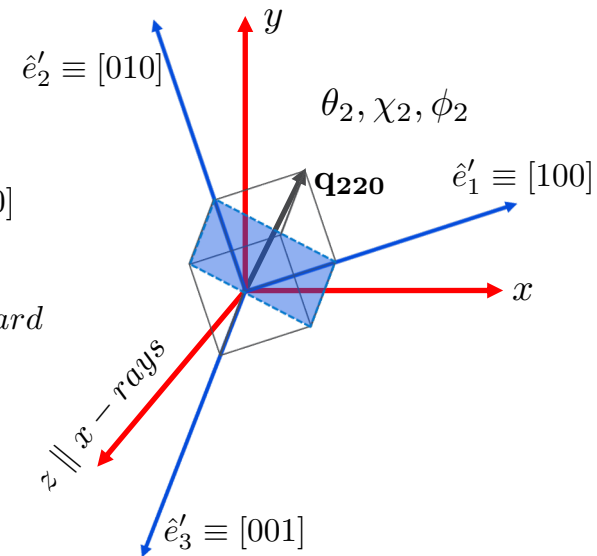
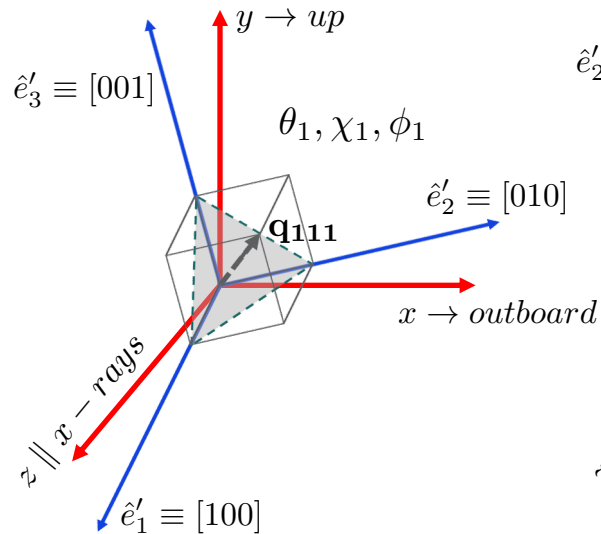
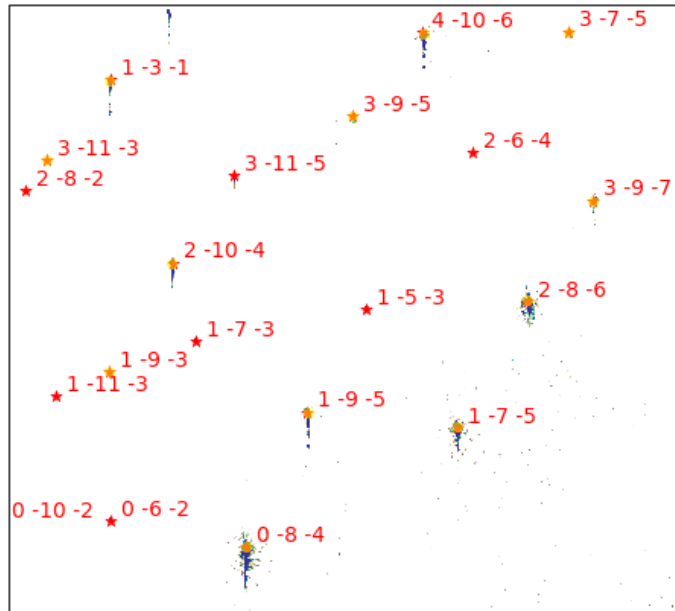
(final - initial) --> $\Delta\mathbf{R}=\{0.0076, -0.0026, 0.0053\}$, $\Delta\mathbf{P}=\{0.379, 0.501, -0.488\}$

(hkl) after E-cal	(hkl) before E-cal	Px	Py	E-measured [keV]
(1-11)	(111)	163	204	2.588 (12.94/5)
(3-53)	(335)	213	490	13.1
(5-53)	(535)	363	293	12.32
(3-55)	(355)	59	376	13.66
(7-55)	(755)	293	62	13.635

Laue orientation 0.7 degree error!

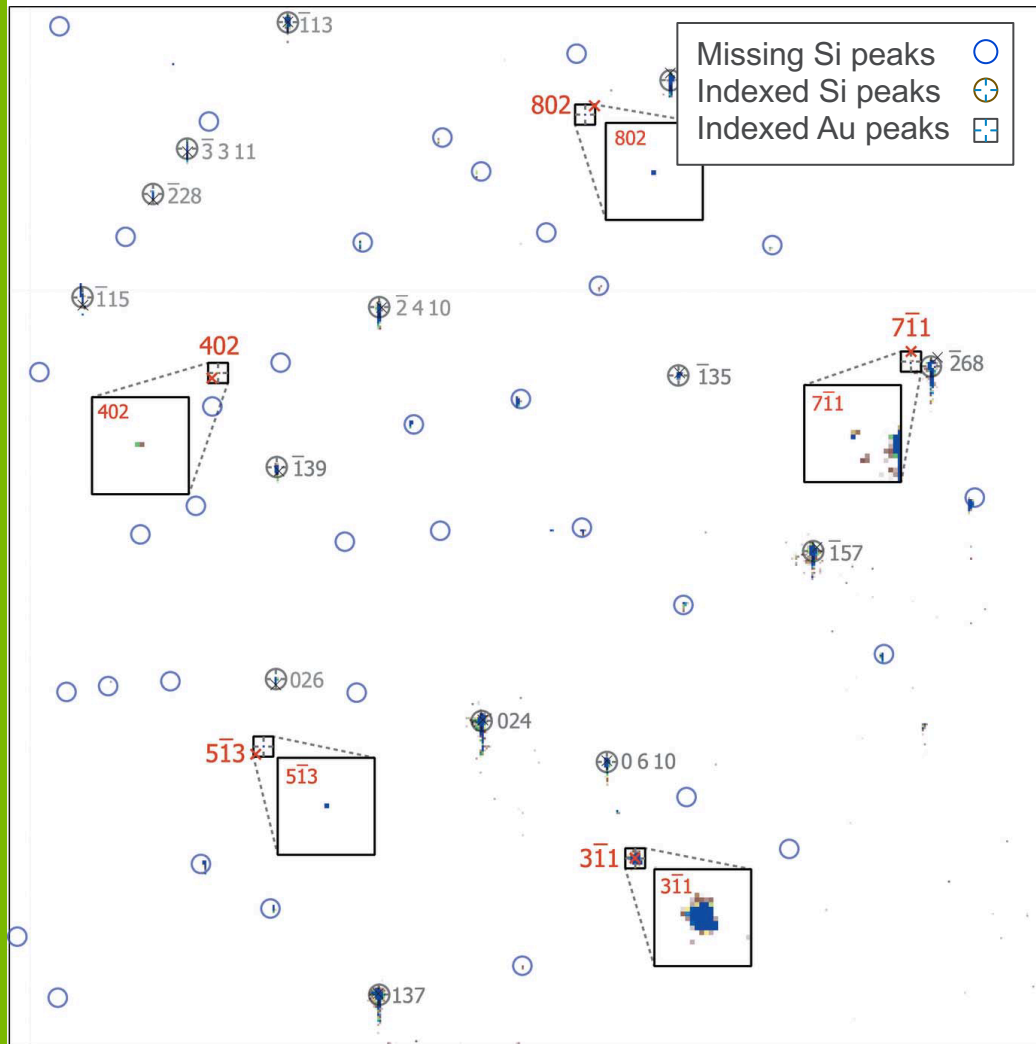
Laue Detector Calibration with Two Bragg Peaks

1. Determine sample orientation by locating two Bragg peaks on diffractometer.
2. Forward model Laue pattern with known sample orientation.
3. Nelder-Mead multiple parameter optimization for Laue detector
4. Reduced sample orientation error to 0.04 deg. with Laue

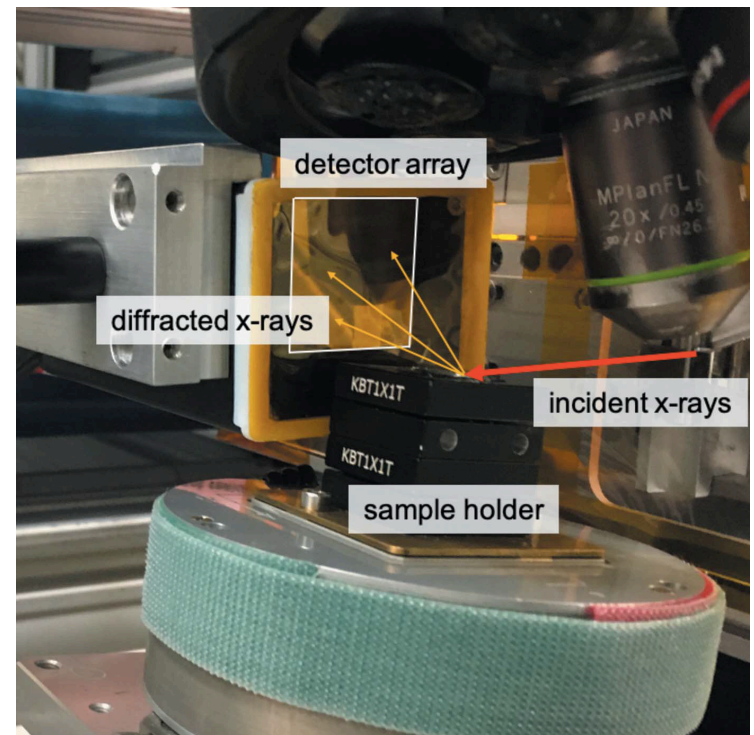


Zhang *et al.* (in preparation)

Laue diffraction @34-ID-C



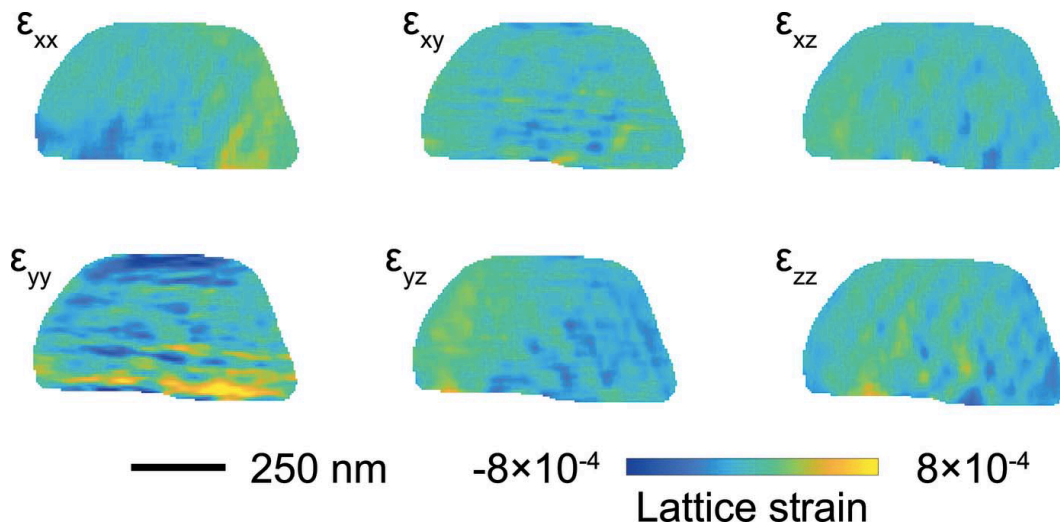
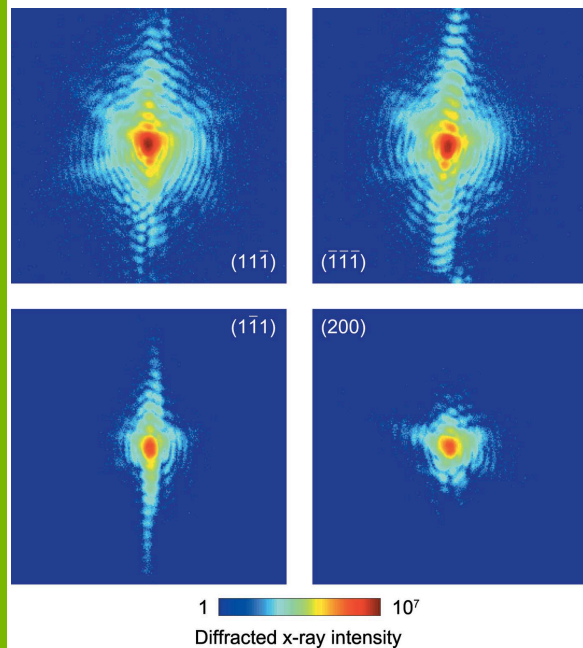
Gold on Silicon



Pateras et al. *J. Synchrotron Rad.* **27** 1430-1437 (2020)

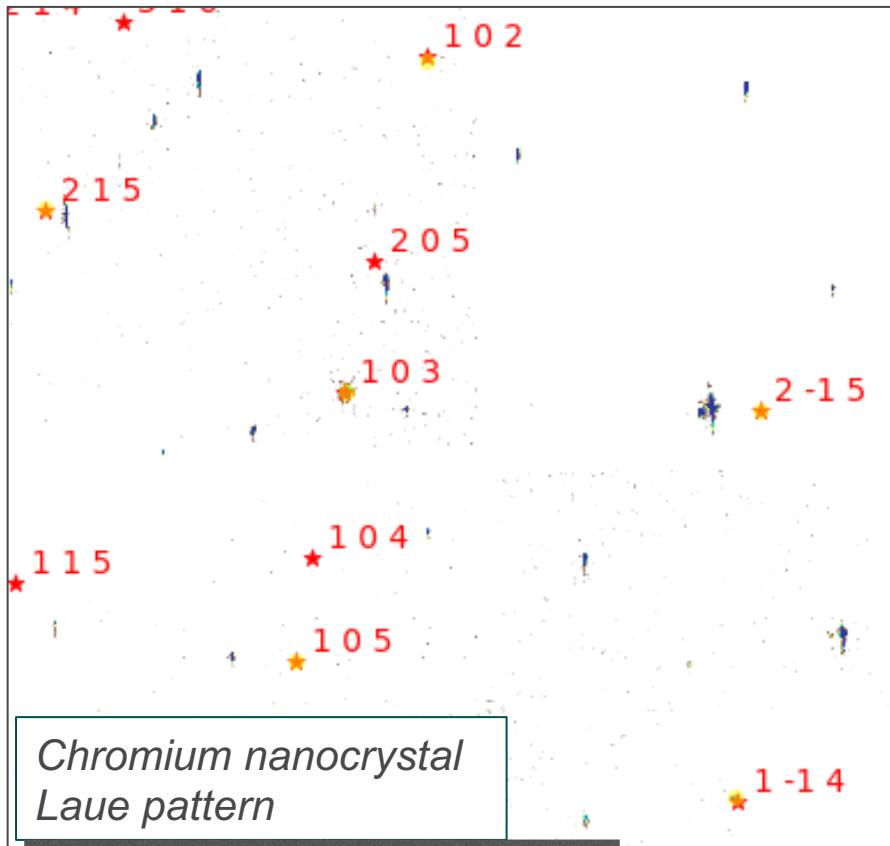
Multi-reflection BCDI

- Independently reconstructing the phases from each Bragg peak
Hoffman et al. *J. Synchrotron Rad.* **24**, 1048-1055 (2017)
- Volumetric full strain tensor



Pateras et al. *J. Synchrotron Rad.* **27** 1430-1437 (2020)

Maturing into a user tool Courtesy Dr Ericmoore Jossou and Dr. Simerjeet Gill (BNL)



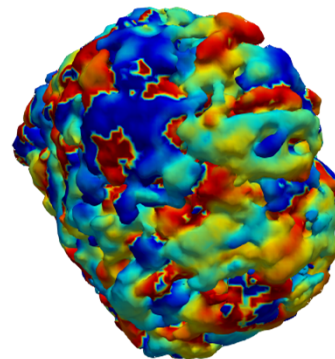
*Chromium nanocrystal
Laue pattern*

1. Algorithms for automatic blob finding
2. Procedures for peak sorting
(Sample vs. substrate peaks)

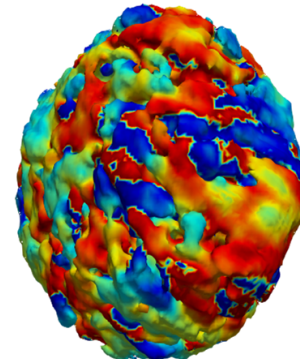
(hkl)	Error (deg.)
(1 0 2)	0.063
(1 0 3)	0.040
(1 0 5)	0.031
(1 -1 4)	0.079
(2 1 5)	0.030
(2 -1 5)	0.003



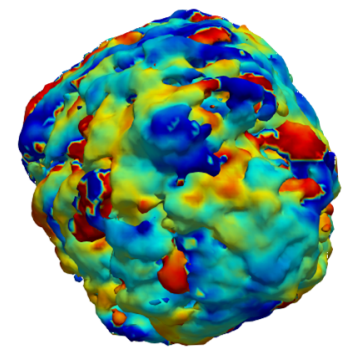
0-1-1



1-10



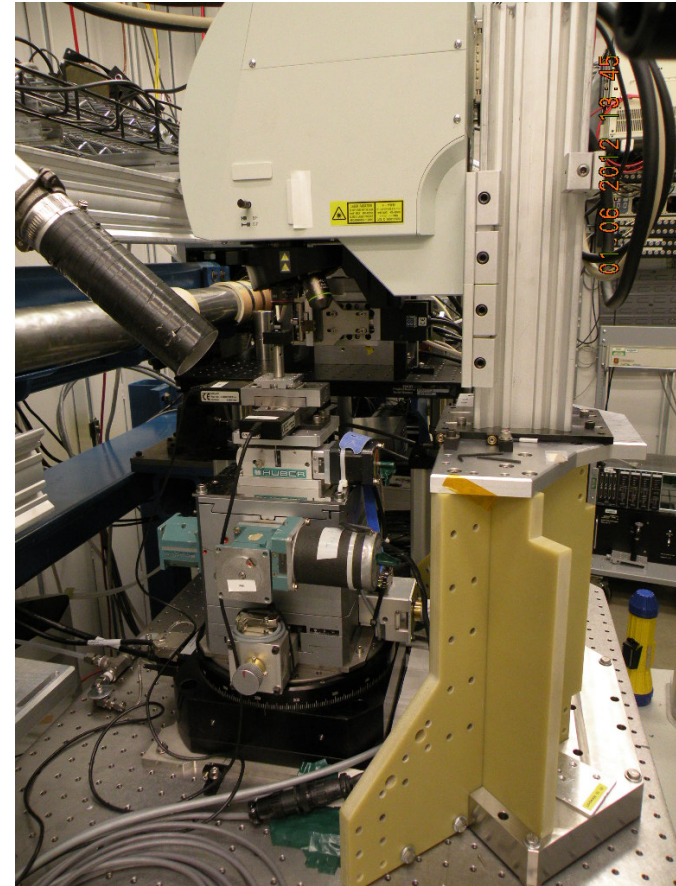
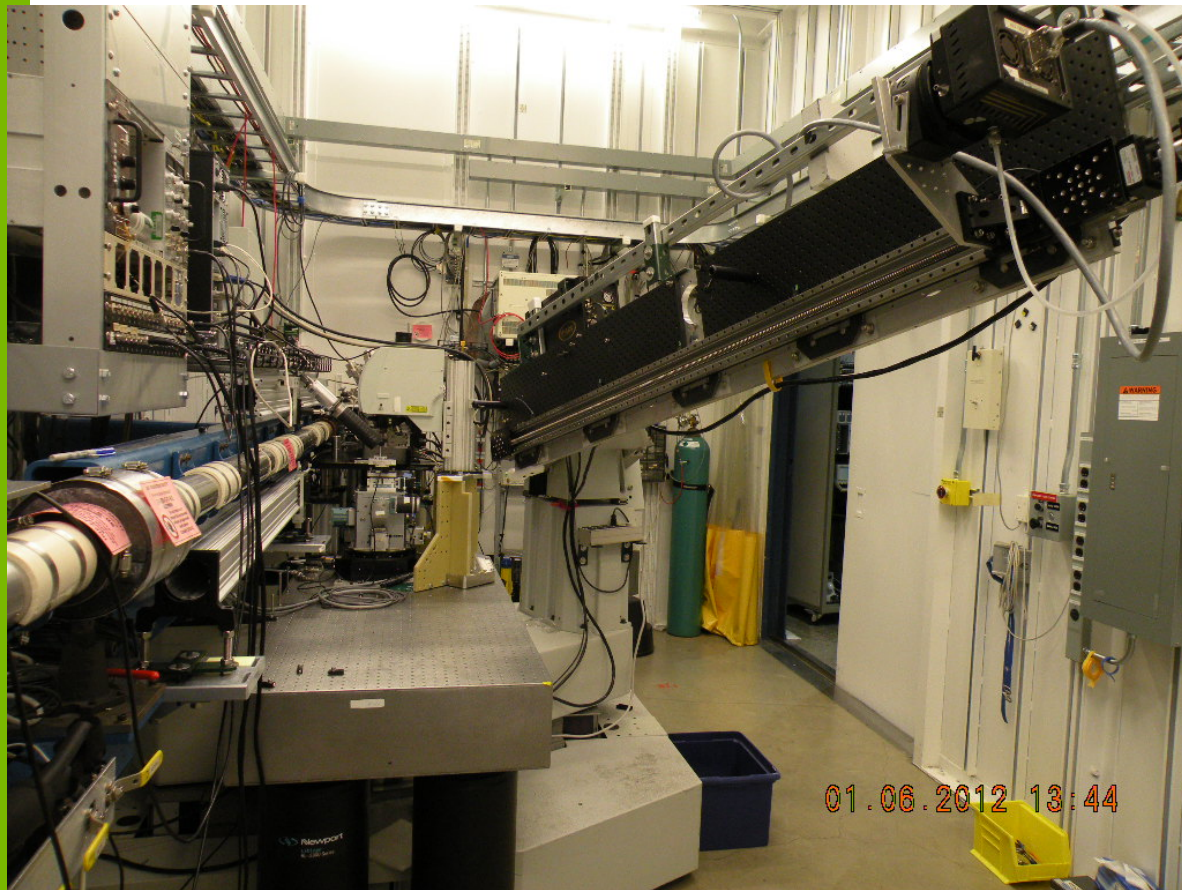
101



APPLY FOR BEAMTIME @ 34-ID-C!

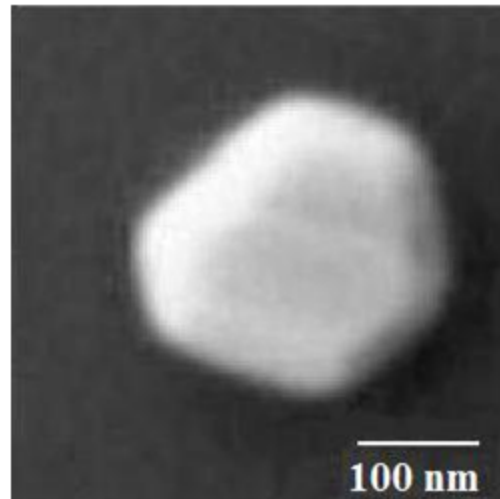
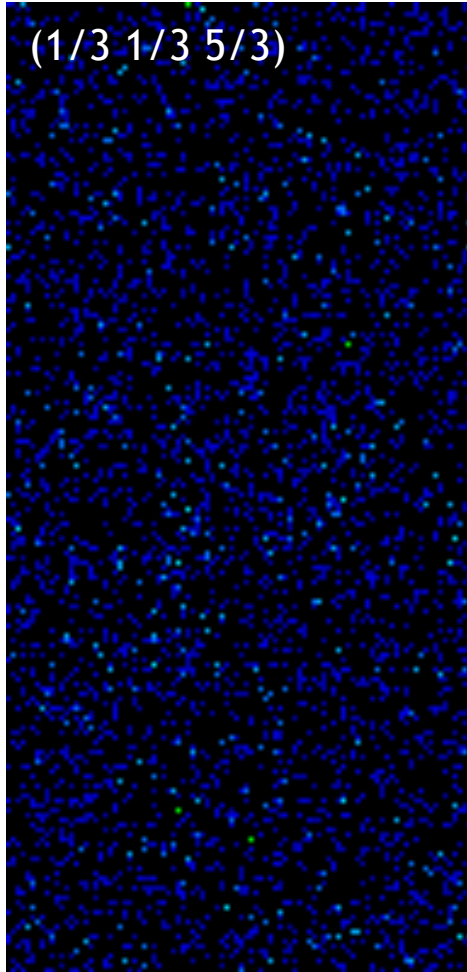
EMAIL: RHARDER@ANL.GOV OR WCHA@ANL.GOV

<https://wiki-ext.aps.anl.gov/s34idc>

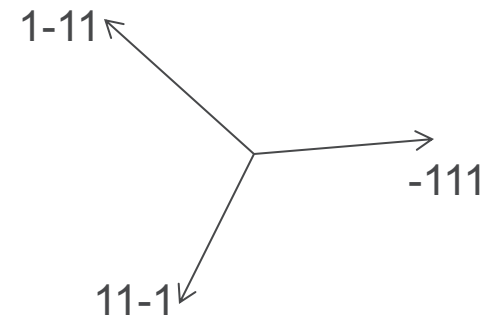
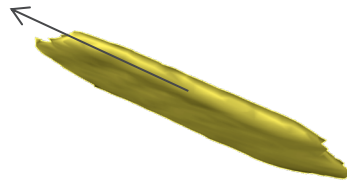


<https://www.aps.anl.gov/>

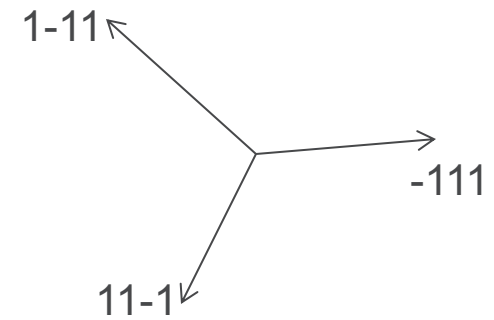
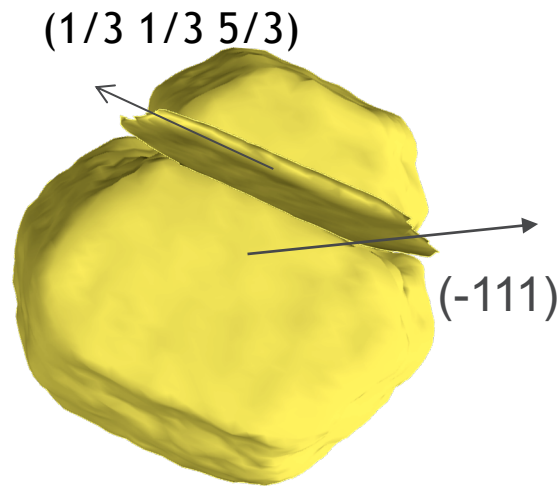
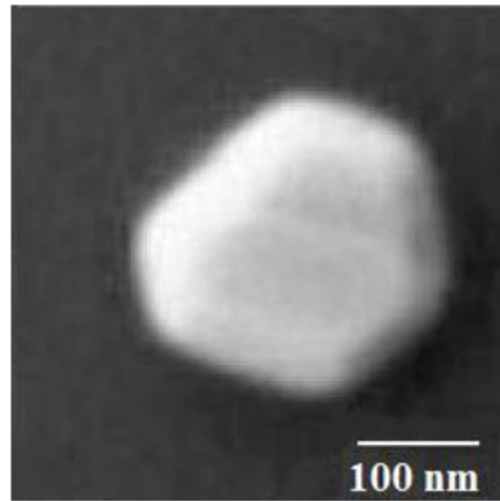
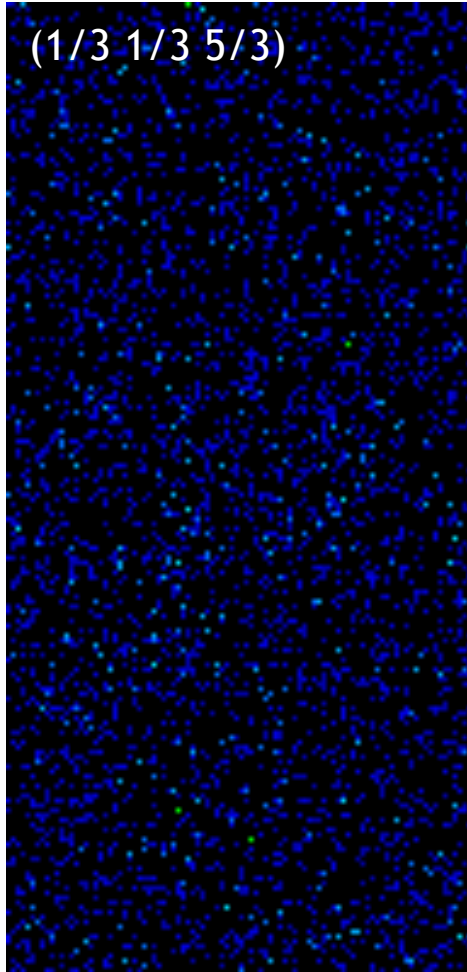
Multiple reflection reconstructions



$(1/3 \ 1/3 \ 5/3)$



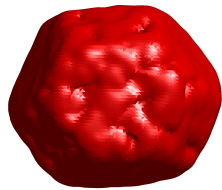
Multiple reflection reconstructions



3D LATTICE DISTORTIONS AND DEFECT STRUCTURES IN ION-IMPLANTED NANO-CRYSTALS.

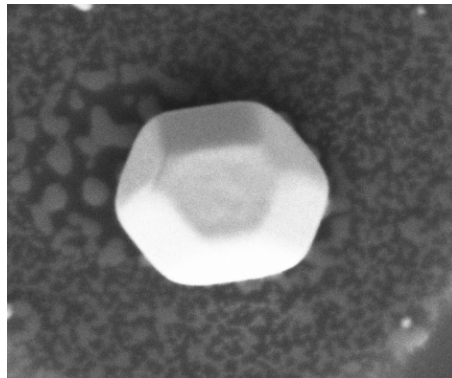
HOFMANN, F. *ET AL. SCI REP* 7, 45993 (2017).

BCDI reconstructed morphology



1 μm

Scanning electron micrograph



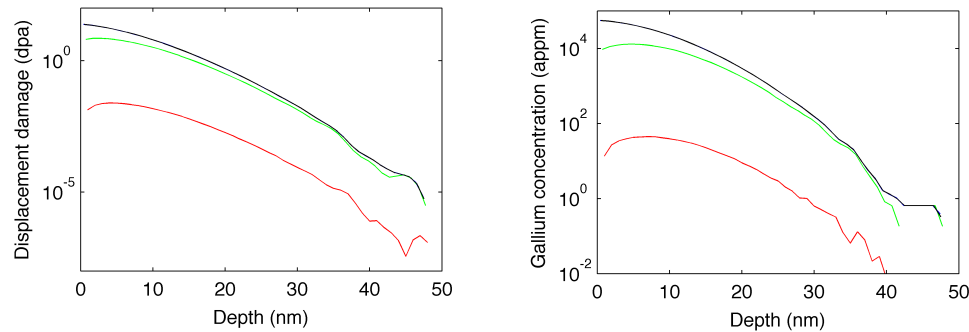
FIB milling conditions:

- 30 keV Ga⁺
- 50 pA
- 1.5×10^8 ions/ μm^2

This causes (SRIM calculation):

- ~20 nm thick damaged layer
- max. ~24 dpa
- max. ~0.054 at. fr. Ga
- ~40 nm Au removed by sputtering

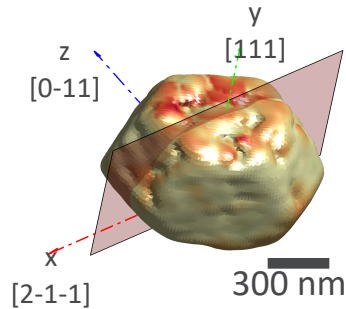
SRIM-predicted damage and Ga concentration



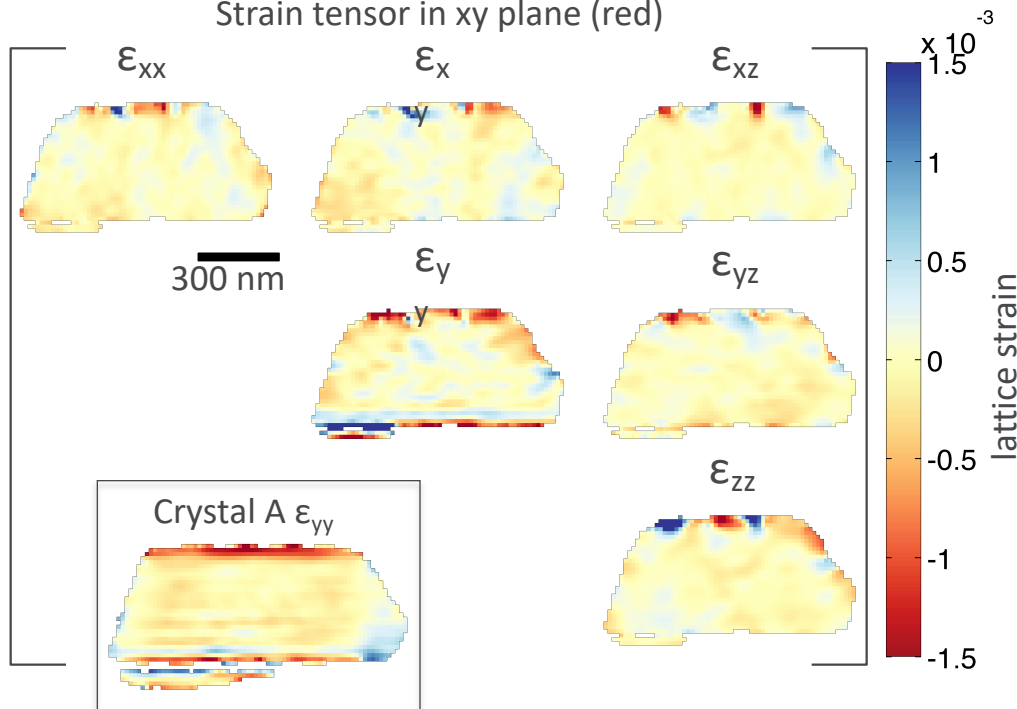
— Crystal A — Crystal B — Crystal C — Crystal D (hole)

3D LATTICE DISTORTIONS AND DEFECT STRUCTURES IN ION-IMPLANTED NANO-CRYSTALS.

HOFMANN, F. *ET AL. SCI REP* 7, 45993 (2017).



Strain tensor in xy plane (red)

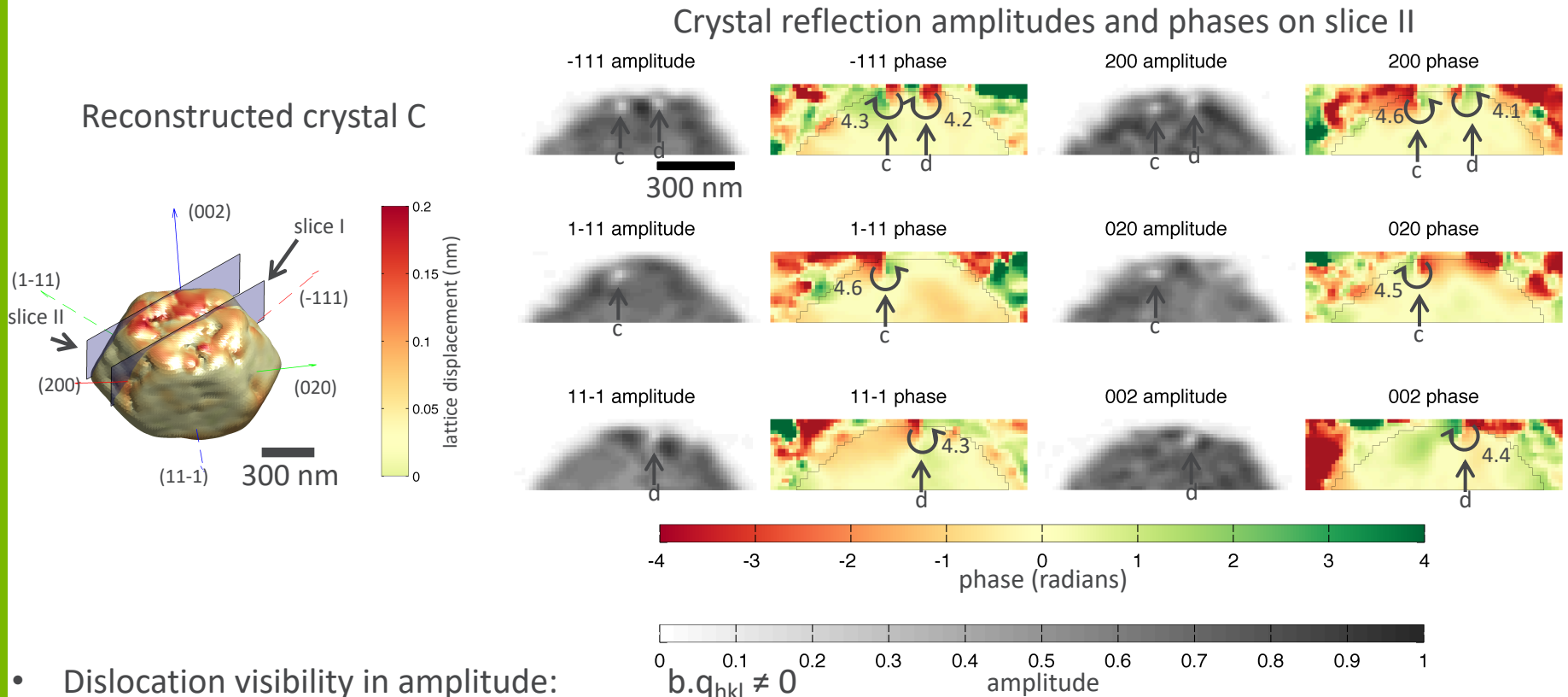


- Non-uniform ϵ_{yy} strain in implanted layer.
- Large positive and negative strains also in all other strain components.

Very different from ion imaged crystal

3D LATTICE DISTORTIONS AND DEFECT STRUCTURES IN ION-IMPLANTED NANO-CRYSTALS.

HOFMANN, F. *ET AL. SCI REP* 7, 45993 (2017).



- Dislocation visibility in amplitude:

$$b \cdot q_{hkl} \neq 0$$

- Phase jump in Burgers circuit:

$$\Delta\psi_{hkl} = b \cdot q_{hkl}$$

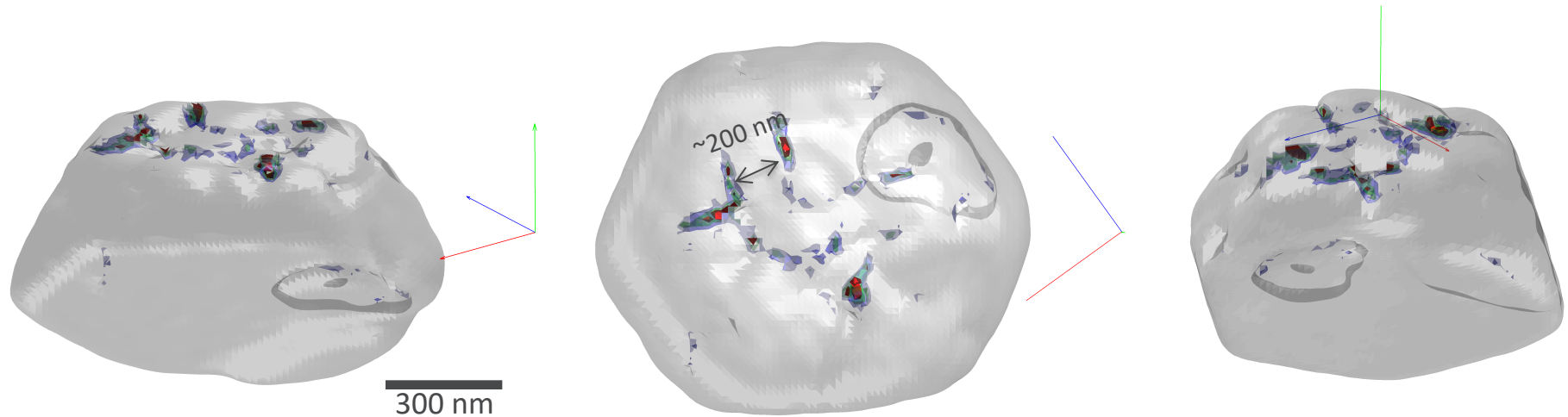
- Defects are stair-rod dislocations with $b = a/3\langle 110 \rangle$

- > Formed by interaction of 2 Shockley partials e.g. $a/6[21-1] + a/6[-21-1] \rightarrow a/3[01-1]$

- > Sessile hence retained?

3D LATTICE DISTORTIONS AND DEFECT STRUCTURES IN ION-IMPLANTED NANO-CRYSTALS.

HOFMANN, F. *ET AL. SCI REP* 7, 45993 (2017).



- Visualisation of 3D dislocation structure by plotting von Mises stress (300 Mpa (blue), 400 Mpa (green), 500 Mpa (red))
- Length scale of dislocation spacing ~ 200 nm
- A simple solution to biharmonic equation, $\Delta^2 \mathbf{u}(\mathbf{r}) = 0$, admissible only at free surfaces, is: $u_y(\mathbf{r}) = A \sin(kx) \exp(-ky)$, $u_x(\mathbf{r}) = u_z(\mathbf{r}) = 0$
- $k = 0.03 \text{ nm}^{-1}$ gives a good fit to the depth-dependent strain due to FIB milling.
-> The associated lateral lengthscale is $L = 2\pi/k = 210$ nm

Simple model provides remarkably good estimate of dislocation self-organisation length scale!